Universidade Federal do Rio Grande – FURG

Instituto de Oceanografia

Programa de Pós Graduação em Oceanologia

Influência da hidrodinâmica nas florações de cianobactérias na Lagoa dos Patos, RS

Beatriz Feltrin Canever

Dissertação apresentada ao Programa de Pós Graduação em Oceanologia, como parte dos requisitos para a obtenção do Título de Mestre.

Orientador: *Prof. Dr. João Sarkis Yunes*

Universidade Federal do Rio Grande (FURG), Brasil

Co-orientadora: *Prof.ª Dr.ª Elisa Helena Leão Fernandes*

Universidade Federal do Rio Grande (FURG), Brasil

Rio Grande, RS, Brasil

Novembro, 2021

Influência da hidrodinâmica nas florações de cianobactérias na Lagoa dos Patos, RS

Dissertação apresentada ao Programa de Pós Graduação em Oceanologia, como parte dos requisitos para a obtenção do Título de Mestre

por

Beatriz Feltrin Canever

Rio Grande, RS, Brasil

Novembro, 2021

Canever, Beatriz Feltrin

Influência da hidrodinâmica nas florações de cianobactérias na Lagoa dos Patos, RS/ Beatriz Feltrin Canever – Rio Grande: FURG, 2021. P. 107 Dissertação (Mestrado) – Universidade Federal do Rio Grande. Mestrado em Oceanologia. Área de Concentração: Física dos Oceanos e Clima.

1. Cianobactérias. 2. Florações de algas nocivas. 3. Hidro dinâmica 4. NDCI. 5. TELEMAC-3D. I. Influência da hidrodinâmica nas florações de cianobactérias na Lagoa dos Patos, RS

“Lo duca e io per quel cammino ascoso
intrammo a retornar nel chiaro mondo;
e sanza cura aver d’alcun riposo,
salimmo sù, el primo e io secondo,
tanto ch’i’ vidi de le cose belle
che porta ‘l ciel, per um pertugio tondo.
E quindi uscimmo a riveder le stelle.”
Dante Alighieri

Agradecimentos

Agradeço primeiramente a Deus e a Nossa Senhora de Lourdes. Agradeço a minha família pelo apoio durante todo o processo. A Gabrielle pelo apoio a distância. A Chariane pela companhia no LCF. A Bruna pela companhia no LANSD. As meninas que me fizeram companhia em Rio Grande: Nadyne, Amanda, Isabella, Vicky e Charlote.

Agradeço aos amigos que me ajudaram durante o mestrado, mesmo que os caminhos divergiram para novas experiências.

Agradeço a CAPES pela determinação de terminar o mestrado. Ao meu orientador e coorientadores: João, Elisa e Wiliam (*in memoriam)* por terem me auxiliado nesse processo.

A Eliana, Felipe, Pablo e Márcio, por terem participado desta empreitada.

Ao meu aplicativo de meditação, amigurumis e livros que me distraíram durante os momentos de ansiedade. A pessoa que sintetizou a bupropiona. As playlists de foco do spotify.

Índice

Lista de Figuras Dissertação

Lista de Figuras Manuscrito 1

Lista de Figuras Manuscrito 2

Lista de Tabelas Dissertação

Lista de Tabelas Manuscrito 1

Lista de Tabelas Manuscrito 2

Lista de Acrônimos e Abreviações

A

ANA – Agência Nacional de Águas

C

CyanoHABS – *Harmful Cyanobacterial Bloom*

E

ECMWF – *European Centre for Medium-Range Weather Forecast*

ENSO – *El Niño Southern Oscillation*

H

HAB – *Harmful algal bloom*

HYCOM – *Hybrid Coordinate Ocean Model*

M

MODIS – *Moderate Resolution Imaging Spectroradiometer*

N

NDCI – *Normalized Difference Chlorophyll Index*

NOAA – *National Oceanic and Atmospheric Administration*

O

ONI – *Oceanic Niño Index*

R

RMAE – *Root Mean Absolute Error*

RSME – *Root Mean Square Error*

Resumo

Florações de algas nocivas afetam negativamente a economia, o turismo e a saúde humana e animal. As mudanças climáticas e a eutrofização tendem a aumentar os riscos destas florações, porém pouco se sabe sobre a influência desses fatores para a região da Lagoa dos Patos. Florações de cianobactérias tóxicas existem na Lagoa dos Patos naturalmente, e são registradas desde o começo do século XX, aparecendo todo verão. Durante o verão de 2019/20 duas manchas de florações foram observadas no corpo lagunar, entretanto, o monitoramento das florações é dificultado pelo tamanho da lagoa, métodos tradicionais de coleta de dados demandam tempo e recursos financeiros extensivos, o que nem sempre é possível. Desta maneira, dois métodos indiretos de coleta e análise de dados foram utilizados para acompanhar as florações de cianobactérias: sensoriamento remoto e modelagem numérica. [Manuscrito I] Para a análise do verão de 2019/20 foi utilizado um índice de clorofila a, NDCI (Normalized Difference Clorophyll Index), comparado com o vento, descarga fluviais e temperatura da água. Dados de precipitação e temperatura do ar foram comparados com uma série histórica, para caracterizar o verão em um cenário de mudanças climáticas. [Manuscrito II] Uma série de verões de 2008 a 2017 foi simulada utilizando o modelo hidrodinâmico TELEMAC-3D acoplado a um módulo lagrangeano para calcular a exportação de cianobactérias para a costa adjacente à lagoa e a acumulação dentro da porção límnica da Lagoa dos Patos. Os verões simulados foram classificados de acordo com o Oceanic Niño Index (ONI) e comparados entre si para entender melhor o efeito do ENSO (El Niño Southern Oscilation) sobre a localização das florações. [Manuscrito I] O verão de 2019/20 foi um verão mais seco que a média climática, o que permitiu o desenvolvimento das florações observadas. Os valores de NDCI representaram a biomassa das duas florações, particularmente em janeiro de 2020. A baixa precipitação e descarga fluvial pode ter influenciado o aumento do tempo de residência da lagoa. Sugere-se que os ventos intensos foram responsáveis pela acumulação das florações nos dias anteriores às manchas observadas ventos de baixa intensidade permitiram o desenvolvimento da floração nas margens. [Manuscrito II] Os verões com maior exportação de cianobactérias foram os

verões de El Niño (2009/10 e 2015/16), opostos aos verões de La Niña (2008/09, 2010/11 e 2011/12). A acumulação das cianobactérias dentro da Lagoa dos Patos foi modulada pelo vento, com ventos de nordeste acumulando as colônias na margem oeste, enquanto ventos do quadrante sul acumularam as florações na margem leste. Os resultados obtidos pelas simulações serão utilizados como modelo de circulação das cianobactérias durante o verão na Lagoa dos Patos, ao fim de monitoraros locais indicados como mais suscetíveis a acumulação das florações.

Palavras-Chave: Cianobactérias, Florações de algas nocivas, Hidrodinâmica, NDCI, TELEMAC-3D.

Abstract

Harmful algal have negative effects on the economy, tourism, and human and animal health. Climate change and eutrophication tend to enhance these risks; however, little is known about the influence of this factors in Patos Lagoon. Cyanobacterial harmful bloom occurs naturally on Patos Lagoon, since the beginning of the 20th century, occurring during summer. During the summer of 2019/20, two bloom patches were observed on the lagoon. However, monitoring the blooms inside the lagoon can be difficult due to the lagoon size as traditional sampling methods are an obstacle because demand extensive financial and time resources. For this reason, two indirect methods for sampling and data analyze were used to investigate the cyanobacterial blooms: remote sensing and numerical modeling. [Manuscript 1] For the summer of 2019/20 an index of chlorophyll a, NDCI (Normalized Difference Clorophyll Index), was compared with winds, river discharge and water temperature. Rainfall and air temperature data were compared with historical data to characterize this summer in a climate change scenario. [Manuscript 2] A series of summers from 2008 to 2017 was simulated using the hydrodynamical model TELEMAC-3D coupled with a lagrangian module to calculate the cyanobacteria export to the adjacent coast of the lagoon, and accumulation inside the limnic section of Patos Lagoon. The simulated summers were classified according to the Oceanic Niño Index (ONI) and compared with each other to better understand the ENSO (El Niño Southern Oscillation) effect on the bloom's location. [Manuscript 1] The summer of 2019/20 was dryer than the climatic average, which allowed the development of the observed blooms. The NDCI values represented booth bloom's biomass, particularly during January/2020. Low rainfall and river discharge might have influenced the high lagoon residence time. We suggest that intense winds were responsible for the bloom accumulation on the days before the observed blooms, and low-intensity winds allowed the bloom development in the margins. [Manuscript 2] The summers with higher cyanobacterial export were classified as El Niño (2009/10 and 2015/16), on the other hand, La Niña summers (2008/09, 2010/11 and 2011/12) had the opposite result. The cyanobacteria accumulation inside Patos Lagoon was modulated by winds, with Northeast winds accumulating the colonies in the Western margin, while Southern winds

accumulated the blooms on the Eastern margin. The simulation results presented here will be used as a cyanobacterial circulation model during the summer on Patos Lagoon to assist monitoring the places susceptible to blooms accumulation.
Keywords: Cyanobacterial, Harmful algal blooms, Hydrodynamics, NDCI, TELEMAC-3D

Capítulo I: Introdução

Florações de cianobactérias nocivas (cianoHABs) são uma preocupação crescente no mundo inteiro devido as consequências negativas na economia, turismo e uso da água. Além disso, a eutrofização e as mudanças climáticas tendem a aumentar a sua incidência e potencializar os efeitos negativos associados a elas [Reichwaldt and Ghadouani, 2012, Paerl, 2017].

Microcystis é uma cianobactéria potencialmente tóxica, que possui como metabólito secundário a microcistina, uma hepatotoxina prejudicial as diversas espécies presentes na água e animais terrestres, como humanos [Carmichael, 1994, Matthiensen et al., 2000]. É o gênero de cianobactéria mais presente nas florações de climas temperados [Howard, 2001], e apesar de nem todas as cepas produzirem toxinas, as cepas tóxicas tendem a dominar durante a floração [Kardinaal et al., 2007]. Estas cepas apresentam condições ótimas de crescimento em temperaturas acima de 20ºC e pH em torno de 8, o que acontecem anualmente na Lagoa dos Patos durante o verão [Yunes, 2009].

Por estar localizada no sul do Brasil, a lagoa sofre os efeitos da oscilação sul do El Niño (ENSO), com anomalia positiva de precipitação durante os episódios de El Niño e anomalias negativas durante os episódios de La Niña [Fernandes et

al., 2002; Marques, 2012; Bitencourt et al., 2020a; Távora et al., 2020]. Além da influência na precipitação, e consequentemente, na vazão dos rios, o ENSO também afeta o regime de ventos, aumentando a ocorrência de vento sul durante La Niña. Períodos de El Niño aumentam a diversidade de peixes na região do estuário [Possamai et al., 2018], assim como a exportação de fitoplâncton da porção límnica para o estuário [Odebrecht et al., 2005].

O verão na Lagoa dos Patos é caracterizado por uma menor taxa de vazão dos rios, considerado como a estação seca, em comparação com o inverno [Aguilera et al., 2020]. Os ventos predominantes são de nordeste, e são a forçante dominante, oscilando de acordo com a entrada de frentes [Moller et al., 1996]. Assim, o tempo de residência acaba sendo maior que no inverno, levando mais de 90 dias para uma partícula ser exportada da célula mais ao norte (C1), enquanto no inverno, próximo a desembocadura do rio Guaíba, o tempo de residência é menor que 70 dias [Aguilera et al., 2020].

Apesar da diversa comunidade fitoplanctônica da Lagoa dos Patos, o gênero *Microcystis* gera a maior preocupação devido a hepatoxina produzida pela mesma. Apesar de existir naturalmente na lagoa [Yunes, 2009], o aumento dos eventos extremos, mudanças climáticas e eutrofização pode mudar a ocorrência das espécies fitoplanctonicas locais [Paerl, 2017, de Souza et al., 2018], já que o crescimento das cianobactérias são favorecidas em caso de aumento de períodos de estiagem [Reichwaldt and Ghadouani, 2012]. Desta forma, há uma preocupação com a saúde de turistas que utilizam a Lagoa dos Patos nas férias de verão, além dos moradores locais que dependem economicamente da região [Yunes, 2009]. Em 2003 houveram casos de alergia reportados as autoridades

sanitárias por banhistas da praia do Cassino, adjacente a costa da Lagoa dos Patos [Silva, 2005].

Cepas de *Microcystis* foram coletadas na Lagoa dos Patos e testadas em laboratório. Hepatotoxinas produzidas por *Microcystis* são conhecidas como microcistinas e pode ser bioacumuladas e biomagnificadas na cadeia trófica, gerando mais prejuízo e riscos para as populações dependentes da região [Onyango et al., 2020]. Foram encontradas duas principais formas de microcistina: a D-leu-microcistina-LR e a D-ala-microcistina-LR entre outras [Matthiensen et al., 2000]. Apesar de ser uma cianobactéria de água doce, *Microcystis* pode ser encontrada também em estuários, como já visto na Lagoa dos Patos [Fujita and Odebrecht, 2007]. A presença das toxinas pode ser diretamente relacionada com a densidade e biomassa de cianobactérias, além de possuir uma fase particulada e uma dissolvida, que possui uma meia-vida maior e permanece mais tempo no ambiente [Kim et al., 2021].

Microcystis aeruginosa encontrada na Lagoa dos Patos [Yunes et al., 1998] possui um ciclo de vida sazonal, com diferentes fases morfológicas, como demonstrado por Reynolds et al. [1981]. Sendo assim, durante o verão as colônias encontram-se na superfície [Yunes et al., 1998]. Períodos de seca baixa velocidade de vento favorecem o crescimento de cianobactérias como a *Microcystis*, devido a estratificação [Reichwaldt and Ghadouani, 2012]. Devido a presença de vacúolos de gás, *Microcystis* possui movimentação vertical [Jephcoat and Halliday, 2008], mantendo seu crescimento em águas estratificadas. Outra característica que possibilita a dominância de *Microcystis* na Lagoa dos Patos é sua tolerância a águas salobras, mantendo seu crescimento em águas com salinidade até próximas a 5, ou seja, mesmo sendo

carreadas da parte limnica da lagoa, em eventos de altas descargas fluviais, para o estuário, a cianobactéria continua crescendo, e possivelmente produzindo toxinas, como observado na Lagoa dos Patos por Salomon *et al.*, [2000].

Quando não é transportada para o estuário, a *Microcystis* pode ficar represada, sendo carreada pelo ventos dentro da lagoa, aumentando o risco de produção de toxinas [Matthiessen A., Yunes J. S., 1999; de Souza et al., 2018];

Devido aos danos causados pelas cianoHABs, cada vez mais se torna necessário o monitoramento das manchas com o objetivo de identificar a sua expansão e toxicidade [Lehman et al., 2005, Onyango et al., 2020]. Porém, coletas *in situ* em corpos d'água com grande extensão, como a Lagoa dos Patos, demandam recursos humanos e financeiros de alto custo operacional, e nem sempre é possível manter um monitoramento satisfatório apenas com coletas [Wynne et al., 2011]. Para isso, técnicas de análise indireta estão sendo utilizadas para representação do ambiente e suas variáveis.

Dois métodos de obtenção indireta de dados utilizados amplamente são a modelagem numérica e o sensoriamento remoto. Muitas vezes são utilizados em conjunto, já que os dois métodos se complementam. Enquanto o sensoriamento remoto possibilita a coleta de dados biológicos, a modelagem trabalha com a advecção de fitoplâncton [Wynne et al., 2011, Soontiens et al., 2019].

O sensoriamento remoto utiliza da capacidade da água e de seus constituintes tem de interagirem com a luz. Os principais constituintes são: partículas algais, partículas orgânicas e inorgânicas em suspensão, materiais orgânicos dissolvidos e as partículas da água [Mobley, 1994]. A concentração destes constituintes muda a assinatura espectral, de modo que diferentes regiões

possuem diferentes picos de reflectância, desta forma, as águas costeiras, oceânicas e continentais podem ser classificadas de acordo com suas características sendo refletidas nos perfis de reflectância como apresentado por Spyrakos et al. [2018].

Os pigmentos presentes nas cianobactérias determinam a presença ou ausência de floração na água, porém, a identificação não é específica por espécie, portanto, não é possível identificar florações nocivas apenas com o sensoriamento remoto, sendo necessário monitoramento *in situ* para confirmação das espécies presentes [Caballero et al., 2020].

Diferentes índices de clorofila derivados a partir de dados de sensoriamento remoto foram desenvolvidos para monitorar florações de algas utilizando bandas combinadas [Dall'Olmo and Gitelson, 2005, Mishra and Mishra, 2012].

Modelos matemáticos por sua vez, podem ter configurações específicas sobre espécies, incluindo nas equações variáveis como crescimento populacional e nutrientes. Esses modelos necessitam uma grande quantidade de informações que podem não estar disponíveis [Anagnostou et al., 2017], porém, quando focado na trajetória das colônias, as caraterísticas biológicas podem ser ignoradas pelo modelo, já que as cianobactérias são carreadas pela corrente independente das suas características biológicas, assim, é possível calcular a trajetória, e monitorar a localização da floração, com um menor gasto computacional [Wynne *et al.*, 2011].

Capítulo II: Objetivos

II.1 Objetivo Geral

Avaliar como a dinâmica de ventos e descargas fluviais afeta a distribuição de colônias *Microcystis aeruginosa* na Lagoa dos Patos e áreas adjacentes.

II.2 Objetivos Específicos

Caracterizar as condições meteorológicas na distribuição e acumulação das colônias nos meses de verão na Lagoa dos Patos;

Avaliar os efeitos de eventos de El Niño e La Niña na distribuição das colônias em comparação com um ano neutro;

Determinar sob que condições as colônias de *M. aeruginosa* pode ser exportada para a zona costeira.

Capítulo III: Área de estudo

Localizada entre as entre as latitudes 30º12’–32º12’S, 50º40’–52º15’W, a Lagoa dos Patos possui uma extensão de 250 km, e largura média de 40 km margeando diversas cidades do estado do Rio Grande do Sul [Möller et al., 2001]. Considerada a maior laguna estrangulada do mundo [Kjerfve, 1986], a Lagoa dos Patos possui uma única ligação com o Oceano Atlântico, ao sul da lagoa, com aproximadamente 700m de largura [Möller et al., 2001; Bitencourt et al., 2020b].

Do ponto de vista hidrodinâmico, a lagoa está localizada numa região de micro maré, sendo assim, a influência da maré se resume ao estuário [Möller et al., 2001]. Com isso, as forçantes dominantes nesse corpo d’água são vento e descarga fluvial [Fernandes et al., 2002; Marques, 2012; Möller et al., 2009]. Possui três tributário majoritários: os rios Guaíba e Camaquã e o Canal de São Gonçalo, que liga a Lagoa dos Patos à Lagoa Mirim. Juntos, os três tributários possuem uma vazão média de 2400 $m^{-3}s^{-1}$ [Vaz et al., 2006]. Os ventos são

predominantes de nordeste, porém as maiores intensidades de vento vêm da direção sul. Essa dinâmica entre vento e descarga fluvial afeta diretamente a qualidade de água e a distribuição de clorofila dentro da lagoa [Seiler et al., 2020]

Bortolin et al. [2020**]** dividiu a Lagoa dos Patos em três diferentes células de circulação (C1, C2 e C3) baseado em sua geologia. De acordo com o autor, as margens da lagoa funcionam como depósito de areia, enquanto lamas e argilas se concentram nas áreas centrais devido à baixa velocidade, que proporciona a deposição de sedimentos. Mais informações sobre a área de estudo foram citadas na introdução.

Capítulo IV: Material e Métodos

IV.1 Obtenção das imagens da floração do verão de 2019/2020

As florações observadas no verão austral de 2019/20 foram relatadas ao Laboratório de Cianobactérias e Ficotoxinas por moradores das margens da Lagos dos Patos na região de Tavares (30 de dezembro de 2019) e Arambaré (13 de janeiro de 2020). Fotografias da floração de Tavares foram cedidas por moradores, enquanto as imagens da floração de Arambaré foram obtidas pelo portal de notícias da região (www.cliccamaqua.com.br).

IV.2 Aquisição e processamento dos dados de sensoriamento remoto

Para o cálculo do NDCI (Normalized Difference Chlorophyll Index), foram coletados os dados do satélite Sentinel-2 nas bandas 708 nm e 655 nm com resolução temporal de 3 dias e resolução espacial de 60m. Os dados passaram por correção atmosférica, correção de glint e remoção de nuvens antes da

aplicação da máscara na Lagoa dos Patos. Com isso foi possível calcular os valores de NDCI a partir da equação 1:

$$C_{chl-a} \propto \frac{[R_{rs}(708) - R_{rs}(665)]}{[R_{rs}(708) + R_{rs}(665)]}$$ Equação (1)

Onde: $C_{chl\text{-}a}$ é o valor de NDCI *e* R_{rs} é a reflectância nas bandas 708 e 665.

Após o cálculo, os valores de NDCI foram divididos valores abaixo de 0 (ausência de floração) e acima de 0 (presença de floração). O cálculo e posterior geração dos mapas e gráficos foram realizadas pelo Prof. Dr. Felipe de Lucia Lobo (co-autor do artigo). Uma série temporal de 5 anos foi criada com os dados de NDCI, de janeiro de 2016 a junho de 2020 em quatro áreas da lagoa, cada uma tendo um diâmetro de 5.000 m, com os resultados interpolados utilizando a interpolação cúbica para obtenção de dados diários para 4 pontos(Fig. 1) no centro da Lagoa dos Patos: Arambaré (-31.0349, -051.4253), Centro (-31.3189, -051.4725), Tavares I (-31.1296, -051.2828) e Tavares II (-31.3454, -051.2499).

Complementando os dados de NDCI, dados de temperatura da água foram obtidos pelo MODIS-Terra com resolução temporal diária de 31 de julho de 2019 a 01 de julho de 2020 e resolução espacial de 1 km para os mesmos 4 pontos.

IV.3 Dados meteorológicos, climáticos e descarga fluvial

Os dados de ventos, precipitação e temperatura do ar foram obtidos por meio das estações meteorológicas de Mostardas (margem leste) e Camaquã (margem oeste) com resolução temporal horária. Os dados de precipitação diária foram obtidos pela soma dos dados horários, enquanto os dados de vento e temperatura foram obtidos a partir da média diária.

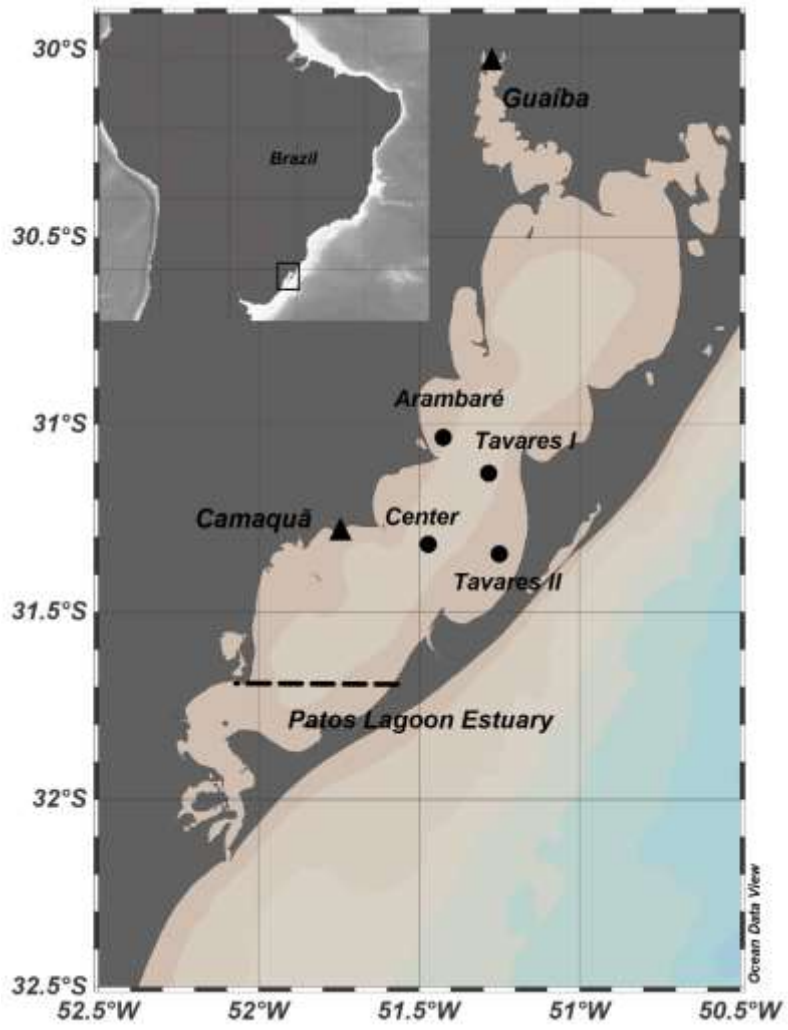

Figura 1. Localização da Lagoa dos Patos. Os triângulos representam os dois principais tributários da lagoa. Os círculos representam os quatro pontos de coleta de dados de temperatura da água e NDCI.

A partir da série histórica organizada e interpolada para o Brasil por Xavier et al. [2016], foram obtidos as médias climatológicas mensais de temperatura do ar e precipitação. Os dados históricos de temperatura (1980 - 2013) foram retirados de um ponto localizado com uma distância de no máximo 1.50º (30º 3’ 0” S, 51º 9’ 36” W) dos 4 pontos relatados anteriormente. Os dados históricos de precipitação (1980 - 2015) foram selecionados de um ponto com uma distância máxima de 0.50º (31º 17’ 24” S, 51º 5’ 44” W) dos mesmos 4 pontos.

A descarga fluvial dos dois principais rios que desaguam na Lagoa dos Patos (Guaíba e Camaquã) foi disponibilizada pela Agência Nacional de Águas (ANA - https://www.snirh.gov.br/hidroweb/download) para o período de 2016 a 2020.

IV.4 Análise dos dados

Os valores de NDCI para o verão de 2019/20 foram relacionados com a temperatura da água, precipitação e direção e velocidade do vento. Os pontos de Arambaré e Centro foram comparados com os dados da estação meteorológica de Camaquã, enquanto os pontos de Tavares I e II foram comparados com os dados da estação de Mostardas. Para a avaliação da interação do vento com as florações, foram calculados os ventos médios dos 5 e 3 dias prévios à floração e os ventos observados no dia da floração.

Os dados de descarga fluvial foram relacionados com o NDCI para o período de 2016 a 2020, relacionando as taxas de vazão com a presença ou ausência de floração. Enquanto os dados de precipitação e temperatura do ar foram utilizados para caracterizar o verão de 2019/2020 em relação aos dados históricos.

IV.5 Modelo hidrodinâmico

TELEMAC-3D (http://www.opentelemac.org) é um modelo matemático que resolve as equações de navier-stokes pelo método de diferenças finitas, considerando a variação local da superfície livre enquanto desconsidera a variação de densidade na equação de conservação de massa. O modelo possibilita os cálculos considerando a pressão hidrostática ou não-hidrostática, utilizando a aproximação de Boussinesq para resolver a equação do movimento. As equações 2-6 são as principais equações resolvidas pelo TELEMAC-3D

Conservação de movimento:

$$\frac{\partial u}{\partial x}+\frac{\partial v}{\partial y}+\frac{\partial w}{\partial z}=0 \qquad \text{Equação (2)}$$

Pressão hidrostática:

$$P=P_{atm}+\rho_0 g(\eta-z)+\rho g\int_z^{\eta}\frac{\Delta\rho}{\rho_0}dz \qquad \text{Equação (3)}$$

Conservação de quantidade de momento:

$$\frac{\partial u}{\partial t}+u\frac{\partial u}{\partial x}+v\frac{\partial u}{\partial y}+w\frac{\partial u}{\partial z}=\frac{-1}{\rho}\frac{\partial P}{\partial x}+V\nabla^2 u+F_x \qquad \text{Equação (4)}$$

$$\frac{\partial v}{\partial t}+u\frac{\partial v}{\partial x}+v\frac{\partial v}{\partial y}+w\frac{\partial v}{\partial z}=\frac{-1}{\rho}\frac{\partial P}{\partial y}+V\nabla^2 v+F_y \qquad \text{Equação (5)}$$

$$\frac{\partial w}{\partial t}+u\frac{\partial w}{\partial x}+v\frac{\partial w}{\partial y}+w\frac{\partial w}{\partial z}=\frac{-1}{\rho}\frac{\partial P}{\partial z}-g+V\nabla^2 w+F_z \qquad \text{Equação (6)}$$

Onde u,vew são as componentes de velocidade dos eixos x,yez, respectivamente; P é a pressão; P_{atm} é a pressão atmosférica; ρ_0 é a densidade inicial da água; ρ é a densidade da água; V é o coeficiente de viscosidade cinemática; g é a aceleração da gravidade; ∇^2é o operador Laplaciano; F_x,F_yeF_z são os termos de fonte horizontais: arrasto do vento, força de Coriolis e fricção do fundo.

O modelo é utilizado para áreas costeiras complexas através do uso de uma malha triangular não-estruturada que permite a criação de elementos de diferentes tamanhos, possibilitando uma malha detalhada próxima a costa e em zonas complexas, enquanto possui uma resolução espacial menor em oceano aberto, diminuindo o tempo computacional e aumentando o detalhamento nas zonas rasas. O modelo 3D é utiliza coordenadas sigma para a discretização vertical.

A lista detalhada com os parâmetros definidos para as simulações está na Tabela 1.

Tabela 1. Parâmetros finais utilizados nas simulações hidrodinâmicas.

Parâmetro	Parametrização/Valor
Coeficiente de Coriolis	-7.70735e-05
Modelo de turbulência horizontal	Smagorinski
Modelo de turbulência vertical	Comprimento de Mistura
Tidal flats	Sim
Passo de tempo	60 s
Lei de fricção de fundo	Nikuradse
Coeficiente de fricção de fundo	1e-05
Coeficiente de influência do vento	3e-06

IV.6 Modelo de traçadores Lagrangianos

O TELEMAC-3D resolve as equações que regem a dinâmica de traçadores ativos e passivos. Traçadores ativos, como temperatura e salinidade, influenciam as variáveis do fluido, como por exemplo a densidade, enquanto traçadores passivos são apenas transportados pelo fluido. O transporte de traçadores passivos, utilizado para representar as cianobactérias é controlado pela advecção, difusão e fontes e sumidouros. A equação 7 rege o movimento conservativo dos traçadores:

$$\partial(\rho T) + divergente$$ Equação (7)

A forma não conservativa dos traçadores (Equação 8):

$$\frac{\partial T}{\partial t} + u\frac{\partial T}{\partial x} + v\frac{\partial T}{\partial y} + w\frac{\partial T}{\partial z} = V_t \nabla^2 T + Q$$ Equação (8)

Onde T é o traçador passivo ou ativo; V_t é o coeficiente de difusão do traçador; t é o tempo; u, vew são as componentes de velocidade dos eixos x, yez, respectivamente; Q é a fonte ou sumidouro do traçador.

IV.7 Condições iniciais e de contorno

Uma malha com 52098 nós e 7 camadas sigmas foi criada para as simulações, com quatro contornos líquidos (Fig. 2): os rios Guaíba e Camaquã, o Canal de São Gonçalo e a borda oceânica. As condições inicias de salinidade foram prescritas na lagoa (0) e no oceano (35) enquanto temperatura inicial foi considerada 24ºC em todo domínio.

Os dados diários vazão dos rios Guaíbas e Camaquã foram retirados do site da Agência Nacional de Águas (ANA - https://www.ana.gov.br). O Canal de São Gonçalo não possui série temporal disponível para o período analisado, portanto foi utilizado a vazão diária média constante de 700 m^3s^{-1} calculada por Vaz et al. (2006).

O contorno atmosférico foi forçado a partir de dados globais com resolução espacial de 0.75º e resolução temporal de 6 horas, disponibilizados pelo ECMWF (*European Centre for Medium-Range Weather Forecasts*, https://www.ecmwf.int). Estes dados foram interpolados para o contorno superficial da malha.

Por fim, o contorno oceânico foi forçado com dados de salinidade e temperatura com resolução espacial de 1/12º e resolução temporal de 3 h, disponibilizados pelo HYCOM+NCODA (*Hybrid Coordinate Ocean Model and Navy Coupled Ocean Data Assimilation,* https://www.hycom.org/). Dados de altura da

superfície do mar e velocidade de corrente de maré são disponibilizadas pelo projeto TPXO, acoplado ao TELEMAC-3D, e foram forçados no contorno oceânico transversal (Fig. 2). Todos os dados forçados no limite oceânico foram interpolados verticalmente, para as 7 camadas sigma.

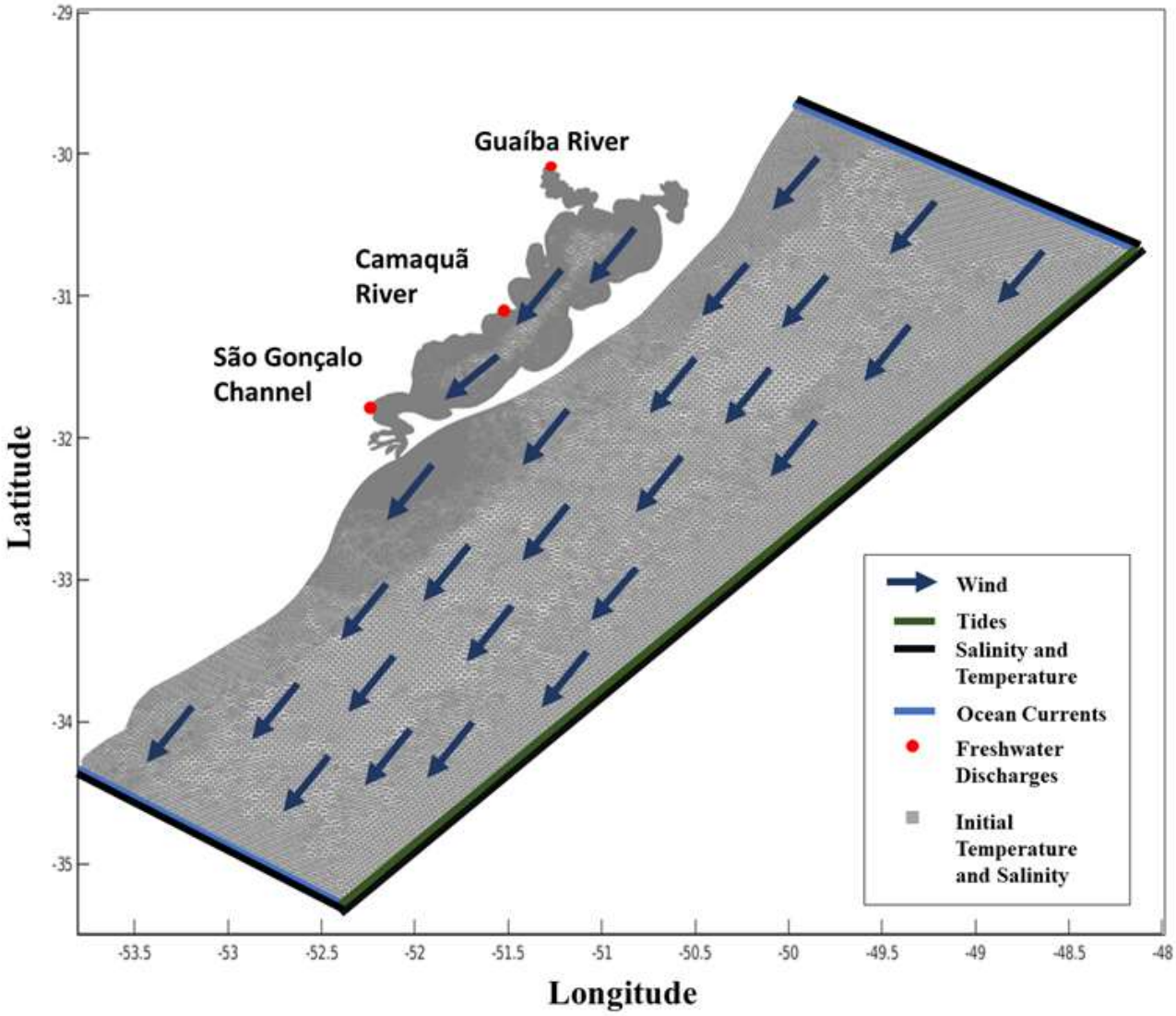

Figura 2. Contornos abertos da malha e suas respectivas condições iniciais e de contorno.

IV.8 Calibração e validação do modelo

Para a comprovação da capacidade do modelo de representar a realidade, foi realizada a calibração e validação dos dados simulados. A calibração foi

realizada por Fernandes et al. (2021) com dados do módulo de velocidade transversal de corrente de superfície e fundo (13 m de profundidade) disponibilizados pela Estação de Praticagem (32° 08' 12" S e 52° 06' 09" W), obtidos por meio de um ADP (*Acoustic Doppler Profiler*) Sontek 1000 Hz para o mês de dezembro de 2011.

A correlação entre os dados simulados e medidos foi calculada a partir dos índices RMAE (*Raiz do Erro Médio Absoluto*) e RMSE (*Raiz do Erro Quadrático Médio*). Enquanto o RMSE informa a magnitude do erro, o RMAE classifica a qualidade dos resultados de acordo com a Tabela 2 [Walstra et al., 2001]. Tanto os valores simulados de superfície quanto o de fundo (13 m) apresentaram resultados excelentes segundo o RMAE (0,06 e 0,14, respectivamente).

Tabela 2. Classificação dos valores de RMAE de acordo com Walstra et al. [2001]

Qualidade do Resultado	Excelente	Boa	Razoável	Pobre	Ruim
RMAE	< 0,2	0,2 – 0,4	0,4 – 0,7	0,7 – 1,0	> 1,0

Ao todo, 45 testes de calibração foram realizados com variação nos valores de coeficiente de difusão horizontal e vertical da velocidade e o coeficiente de atrito do vento. Os valores que apresentaram o melhor resultado (RMSE = 0,31 e 0,19 RMAE = 0,06 e 0,14, superfície e 13 m de profundidade, respectivamente; Fig. 3) foram $3,0*10^{-6}$ para o coeficiente de atrito do vento, 30 para o coeficiente de difusão horizontal e $1,0*10^{-6}$ para coeficiente de difusão vertical.

Para a validação, os dados de salinidade a 4 m de profundidade foram disponibilizados pelo projeto Cassino e Projeto PELD (https://peld.furg.br) para

o ano de 2017. Os resultados obtidos por Fernandes et al. (2021) (Fig. 4) apresentaram boa representação da realidade.

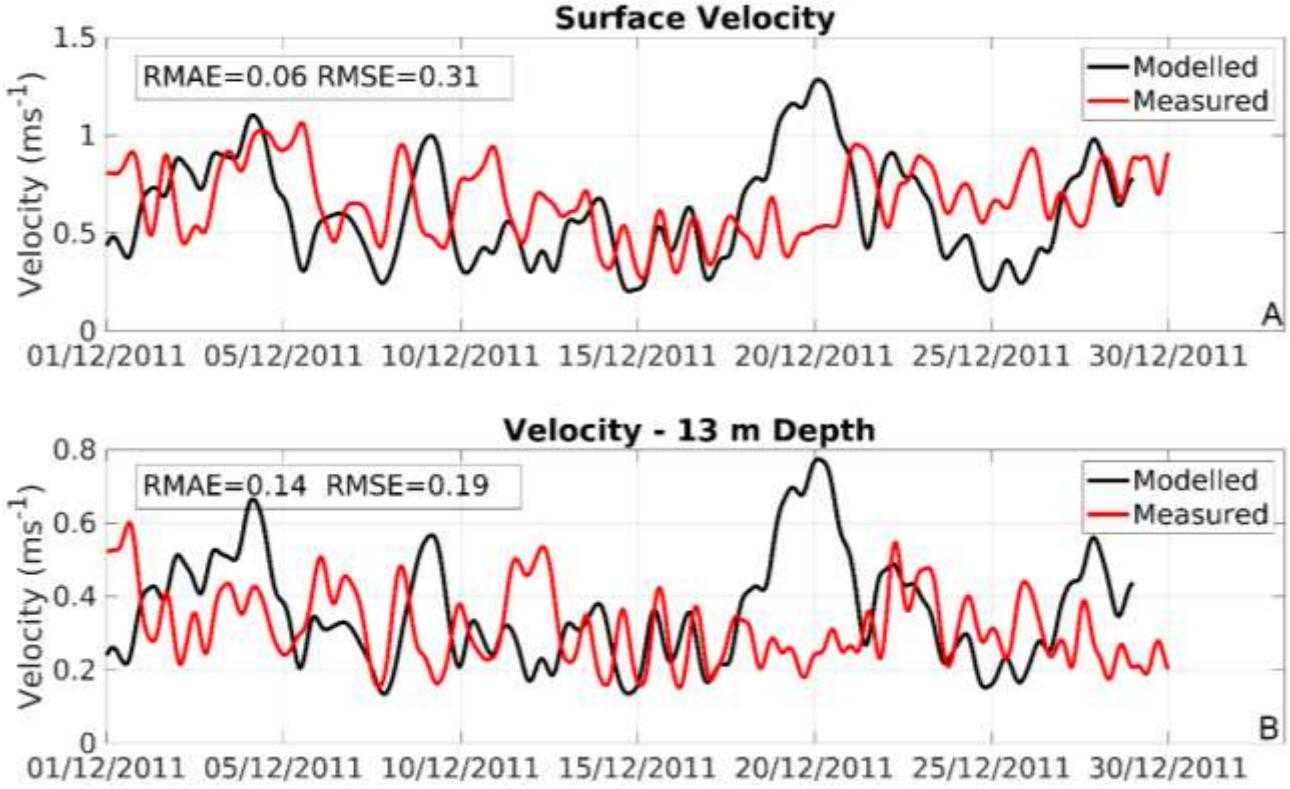

Figura 3. Valores de RMAE e RMSE para velocidade de corrente. Dados modelados em preto e dados medidos em vermelho. A) Superfície, B)13 m. Dados medidos na estação de praticagem. Adaptado de Fernandes et al. [2021].

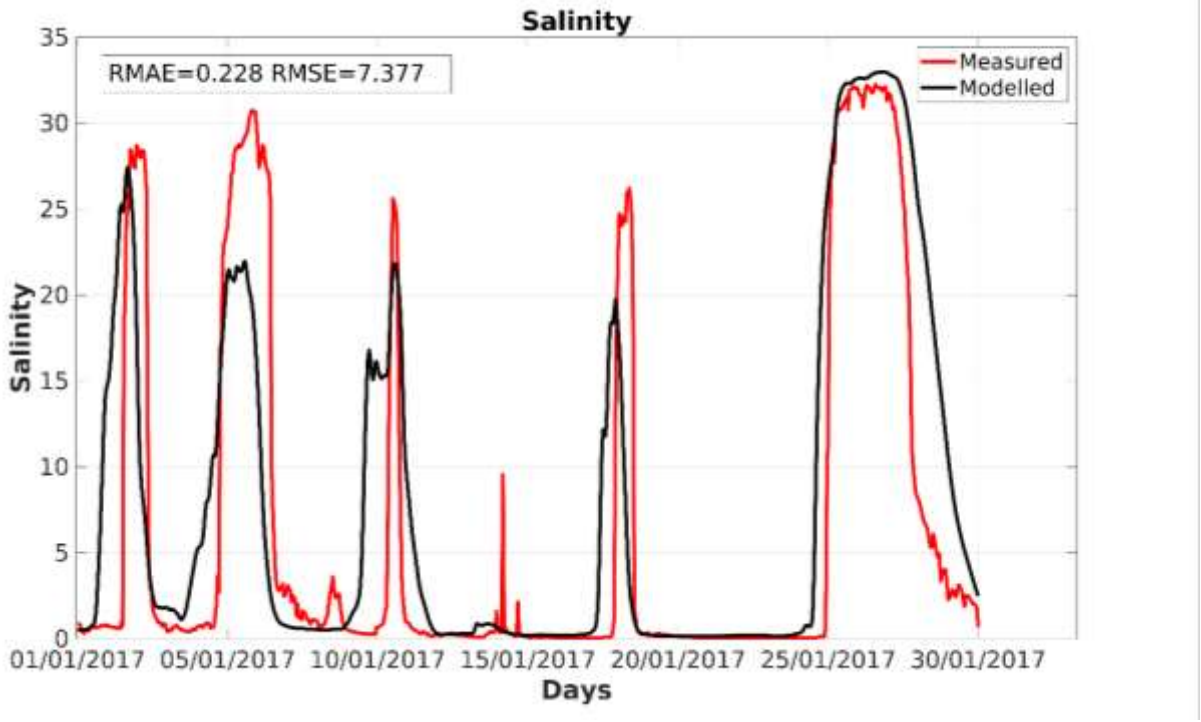

Figura 4. Resultados de RMAE e RMSE para a validação de salinidade a 4 m de profundidade. Dados modelados em preto e dados medidos em vermelho. Adaptado de Fernandes at al. [2021].

IV.9 Simulação da trajetória das colônias

Para simular a influência do ENSO na trajetória das colônias e exportação de cianobactérias na Lagoa dos Patos foram selecionados 9 verões entre os anos de 2008 a 2017, classificados de acordo com o ONI (*Oceanic Niño Index*). Este índice define a classificação dos eventos ENSO a partir de anomalias na região Niño 3.4 (5ºN-5ºS, 120º-170ºW), onde anomalias positivas (negativas) maiores que 0.5ºC indicam eventos de El Niño (La Niña). Dessa maneira, os verões de 2008/09, 2010/11 e 2011/12 são classificados com La Niña, os verões de 2009/10, 2014/15 e 2015/16 são classificados como El Niño, e os verões de 2012/13, 2013/14 e 2016/17 são classificados como neutros.

Todas as nove simulações começaram no primeiro dia de novembro e terminaram no dia 31 de março do ano seguinte. As partículas foram adicionadas

à simulação no dia 1º de dezembro em nove pontos distribuídos pelas três células da Lagoa dos Patos (Fig. 5). Ao todo foram 7056 partículas, divididas igualmente nos nove pontos (784 partículas por ponto) durante o período de 1º de dezembro a 31 de março do ano seguinte. De acordo com o ciclo de vida da *Microcystis aeruginosa* descrito por Reynolds et al. [1981], durante o verão as colônias de *Microcystis aeruginosa* permanecem na superfície, apenas durante o outono e primavera que ocorre o movimento vertical de ressuspensão/afundamento das colônias, respectivamente. Portanto, as partículas utilizadas nas simulações permaneceram na superfície, sem transporte vertical.

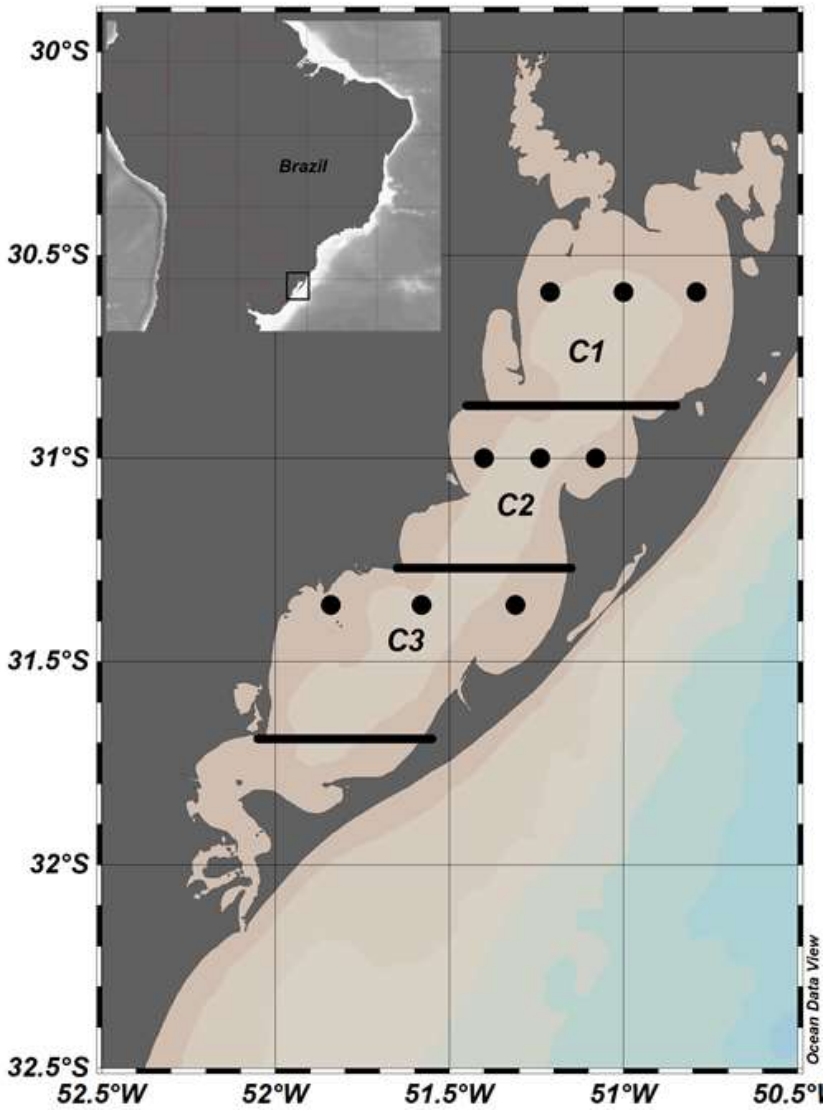

Figura 5. Localização da Lagoa dos Patos separada por células. Os pontos representam a localização inicial das partículas.

IV. 10 Análise dos dados simulados

Com o resultado das simulações foi calculado a exportação de cianobactérias para a costa adjacente a Lagoa dos Patos. Para cada passo de tempo de um dia as partículas dentro e fora da lagoa foram contadas, e ao final da simulação, foi calculado a quantidade de partículas mantidas dentro da lagoa em razão do número total de partículas do último passo de tempo.

A acumulação de partículas na lagoa foi calculada diariamente utilizando um polígono com 2 km de extensão para as margens, divididas entre margem oeste e margem leste para cada uma das três células separadamente. A exportação e acumulação de partículas foi relacionada com vento e descarga fluvial dos rios Guaíba e Camaquã. A vazão do São Gonçalo foi desconsiderada das análises já que é constante independente do cenário, A acumulação de cianobactérias nas margens do estuário não foi analisada, apenas a acumulação dentro das três células.

Capítulo V: Resultados e Discussão: Manuscrito 1

Para a obtenção do título de Mestre pelo Programa de Pós-Graduação em Oceanologia é requerido que o discente realize a submissão de pelo menos um artigo científico como primeiro autor em periódico de corpo indexado. Desse modo, os resultados da pesquisa desenvolvida durante o período de mestrado e a discussão dos resultados serão apresentados em forma de artigo neste Capítulo. O primeiro manuscrito, de autoria de Beatriz Feltrin Canever, Márcio Silva de Souza, Eliana Veleda Klering, Felipe de Lucia Lobo, Elisa Helena Leão Fernandes e João Sarkis Yunes é intitulado: "**Meteorological and potential climatic influence over high cyanobacterial biomass within the Patos Lagoon (southern Brazil): a study case of summer of 2019–2020"** e foi submetido para publicação no periódico "Ocean and Coastal Research".

Meteorological and potential climatic influence over high cyanobacterial biomass within the Patos Lagoon (southern Brazil): a study case of summer of 2019–2020

BEATRIZ FELTRIN CANEVER[1,*], MÁRCIO SILVA DE SOUZA [1], ELIANA VELEDA KLERING[1,2], FELIPE DE LUCIA LOBO[2], ELISA HELENA LEÃO FERNANDES[1], JOÃO SARKIS YUNES[1]

B.F.C.: ORCID® 0000-0002-3770-1113

M.S.S.: ORCID® 0000-0003-1572-9307

E.V.K.: ORCID® 0000-0002-45-08-1997

F.L.L..: ORCID® 0000-0001-8061-0076

E.H.L.F..: ORCID® 0000-0003-1869-0233

J.S.Y.: ORCID® 0000-0002-4792-7626

[1] Instituto de Oceanografia, Universidade Federal do Rio Grande, Av. Itália, km-8, P.O. Box 474, Campus Carreiros, Rio Grande, 96203-900, Rio Grande do Sul – Brazil

[2] Universidade Federal de Pelotas, Pelotas, 96010-610, Rio Grande do Sul – Brazil

* Corresponding author: beatriz.canever@gmail.com

ABSTRACT

Cyanobacterial blooms are a potential threat to human communities and ecosystems. Since the late 80's researchers have reported harmful cyanobacteria colonies in Patos Lagoon, the largest coastal lagoon in South America. Most works concerning harmful blooms in Patos Lagoon focus on its biology and at its southernmost estuarine region, with little information on its displacement inside the lagoon, and the influence of physical forcing on its dynamics. The present study used derived-satellite information (Normalized Difference Chlorophyll *a* Index), river discharges data, and meteorological data (wind speed and direction, rainfall, and air temperature) to analyze two blooms episodes within Patos Lagoon during the austral summer of 2019/2020, specifically in its larger, limnic portion. A 30-year meteorological time series was used to contrast with the same summer period. Two remote sensing images from Sentinel-2 were taken from

both Patos Lagoon margins, near their central portion. The summer of 2019/2020 was drier compared to the historical data, characterizing low river discharge. This environmental condition was coupled with high temperature and thermal stratification that might have promoted cyanobacteria growth and accumulation inside PL. Moreover, weak winds (<<6 ms^{-1}) seemed to accumulate cyanobacteria patches on the water surface, inclusively after vertical mixing caused by strong winds(>>6ms^{-1}). The NDCI values represented well the two days of blooms, with higher values happening under higher water temperatures and low wind speed.

KEYWORDS: FRESHWATER ENVIRONMENT; WIND-DRIVEN HYDRODYNAMICS; RAINFALL; DERIVED-SATELLITE BIOMASS INDEX; CLIMATE VARIATION;

INTRODUCTION

Since cyanobacterial harmful blooms (cyanoHABs) produce cyanotoxins that can cause skin irritations (Paerl and Otten, 2013; Paerl, 2017), they are considered as an over increasing and worldwide threat to the environments and to economic and social activities of human populations, mainly associated with cultural eutrophication and climate change (Paerl and Huisman, 2009, Kennish and Paerl, 2010; King et al., 2015). These photosynthetic microorganisms usually outgrow after the spring (diatom) blooms across many types of aquatic environments, including lakes and lagoons such as Patos Lagoon in southern Brazil (Odebrecht et al., 1987, 2005; Haraguchi et al., 2015).

Several studies have been carried out on the phytoplankton species at a broader sense composed of diatom, green flagellates, cyanobacteria, and other taxonomic groups, particularly in the estuarine part of Patos Lagoon (Haraguchi et al., 2015, and references therein; Mendes et al., 2017). These and other studies have described the relationship between some bio-chemical (inorganic nutrients, salinity) and physical factors (temperature, residence time) (Fujita and Odebrecht, 2007) and at decadal-scale

(Odebrecht et al., 2010; Haraguchi et al., 2015). Cyanobacteria tend to be noticeable during austral summertime and/or follow the decline of other more common phytoplankton groups such as diatoms, within the shallow estuary of Patos Lagoon (Haraguchi et al., 2015, and references therein). Furthermore, the phytoplankton dynamics in that shallow estuary seem to be mainly influenced by wind-driven hydrodynamics in short-term scales (Fujita and Odebrecht, 2007), and by rainfall and drought periods in a seasonal scale (Odebrecht et al., 2010).

However, the major extension of Patos Lagoon is an oligohaline and freshwater system which is still understudied in terms of population dynamics of cyanobacteria. The cyanobacteria dynamics in that limnic system might influence the phytoplankton dynamics further downstream to the lower part of Patos Lagoon and its adjacent coastal area (De Souza et al., 2018) as seen in other estuaries (e.g., San Francisco Bay estuary, Lehman et al., 2005). The link between the limnic and estuarine parts of Patos Lagoon is mainly due to advection processes caused by the continental freshwater contribution and wind forcing (Möller et al., 2001; Möller and Castelo, 2009) in time scales varying from synoptic to interannual (Távora et al., 2020; Bitencourt et al., 2020) since the region is under microtidal influence. Under a summertime scenario of weak winds and low discharges establishing stratification), high surface accumulation of cyanobacteria may be a typical biological feature in freshwater bodies (Paerl and Otten, 2013), as the main symptom of the eutrophication process due to rapid cyanobacteria growth in response to elevated concentrations of nutrients (Cloern, 2001; Paerl, 2017).

Given the potential economic and ecological impacts of cyanoHABs within Patos Lagoon through the limnic area down to its estuarine region and the adjacent coast, it is essential to understand the relation between meteorological driving forces and the movements of high toxic cyanobacterial biomass in the main Patos Lagoon body during

the austral summertime (de Souza et al., 2018; Yunes, 2009 and references therein). This lack of knowledge is important at regional as well as national scales because the northern and central parts of Patos Lagoon serve for agricultural activities, recreational events, and even as drinking water sources for population and livestock animals (Yunes, 2009).

Moreover, it has turned notorious that climate change can be responsible for many environmental and ecological alterations (IPCC, 2021), including the potential of favoring cyanobacteria outbursts and blooms at expense of other phytoplankton species (Paerl, 2017; Paerl et al., 2016). Some important environmental alterations are related to regime shifts in rainfall and dry cycles worldwide (Paerl et al., 2015 and references therein; Thompson, et al., 2015, IPCC, 2021;) and were reported to alter Patos Lagoon continental discharge contribution and wind regime (Távora et al., 2020; Bitencourt et al., 2020). For instance, the alternation between flood and drought events can impact the structure and dynamics of cyanobacteria populations since floods might produce high export rates of nutrients and organic material to adjacent coasts (De Souza et al., 2018). On the other hand, dry periods can result in high phytoplankton biomass (e.g., Lake Erie (Canada-USA): Ho and Michalak, 2017; Michalak et al., 2013), and an increase in residence time (Fernandes et al., 2002; Aguilera et al., 2020), which can promote the development and extension of cyanoHABs in lagoons, such as of the main Patos Lagoon water body.

It is difficult, however, to distinguish between the effects of climate change from the eutrophication influence over the occurrence of cyanoHABs and other HABs across several kinds of water bodies. A manner of reaching that goal is having a time series of meteorological and biotic information, e.g., phytoplankton biomass and composition. But, in lacking *in situ* biotic datasets, one can still retrieve remote sensing-derived

information such as the relative indexes of autotrophic biomass, including cyanobacteria (e.g., Mishra and Mishra, 2012; Mishra et al., 2019; Lobo et al., 2021).

Taking all information above into account, this present work aims to investigate the hypothesis that dry summer periods, particularly an extremely dry year under a climate change context, enhance the frequency and magnitude of cyanobacteria biomass in the limnic part of PL. The investigation will be carried out based on a warm dry period in the austral summer of 2019–2020 that appeared to have promoted high accumulation and growth of cyanobacteria biomass in the limnic and part of PL. A meteorological framework and climatology information (1980–2013; Xavier et al., 2016) will be related with the biological features based on the Normalized Difference Chlorophyll *a* Index (NDCI, see Mishra and Mishra, 2012), considering both margins of the main Patos Lagoon water body (Fig. 1). It is expected that results can be an initial assessment of the relation between the meteorological driving force and cyanoHABs in the limnic area of PL, which will be valuable information for the establishment of monitoring programs and public policy.

METHODS

STUDY AREA

The temperate Patos Lagoon (PL) is part of the Patos–Mirim lagoon system and receives waters from a 200,000 km^2 watershed shared between southern Brazil and northeastern Uruguay (Seeliger 2001; Odebrechet et al., 2010a). Patos Lagoon is the largest lagoonal system in South America (Kjerfve, 1994; Bortolin et al., 2020) and is considered a world natural reserve (Kalikoski and Vasconcellos, 2012). It has one connection with the ocean in its southern part and has three main tributaries: Camaquã

river, Guaíba river, and São Gonçalo Channel (Fig. 1). The region has microtidal-influenced in a way that the circulation of Patos Lagoon is ruled by winds and freshwater discharges (Möller et al., 2001). According to Möller and Castaing (1999) and Távora et al. (2020) flow rates of rivers lower than 2000 m^3s^{-1} also favor wind dominance. Although NE winds are predominant in summer, this season can have a southern wind influence that suppresses export when low rainfall occurs, inducing lower lagoon flow rates (Möller et al., 2009).

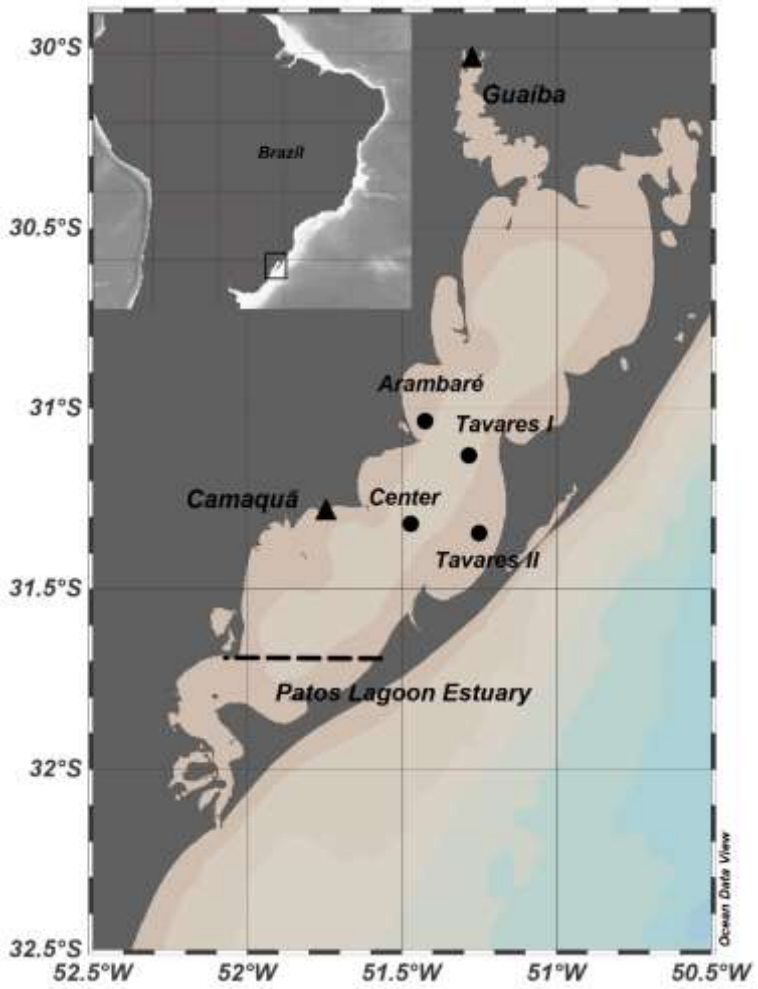

Figure 1: Inset map: Location of the Patos Lagoon in southern Brazil. Main map: Depiction of the four study sites (black circles): Arambaré, Tavares I, Tavares II, and Center; and the two main river tributaries (black triangles), Camaquã and Guaíba. Dashed line delimits the southernmost estuarine portion and the larger limnic portion of the Patos Lagoon.

Some works show the El Niño Southern Oscillation (ENSO) is important on the internal circulation and freshwater export (Möller et al., 2009; Marques, 2012; Távora et al., 2020). El Niño (La Niña) events imply a higher (lower) rainfall rate, therefore, higher (lower) river discharge. The wind pattern also shifts due to ENSO, with La Niña showing more S-quadrant winds, which can contribute to reducing seaward flow. Because of this low discharge and S-quadrant winds, Patos Lagoon has a higher residence time (Fernandes et al., 2002; Aguilera et al., 2020), which might allow the development of freshwater algae and cyanobacteria such as *Microcystis aeruginosa* complex (De Souza et al., 2018) or *Microcystis* spp., *Spirulina* sp. and *Anabaena* (=*Dolichospermum*) spp. (Ferreira et al., 2004).

METEOROLOGICAL AND CLIMATOLOGY DATA, AND RIVER DISCHARGE

In following the casual observations of cyanobacterial blooms next to two cities of the main Patos Lagoon (Fig. 2), meteorological data (air temperature, rainfall, and winds) from INMET (National Institute of Meteorology) stations closer, respectively, to Arambaré (station of Camaquã town) and Tavares (station of Mostardas town) (Fig. 1), were compiled for the time interval of July 2019 to June 2020. At the same time, to contrast that time interval of meteorological events with a mean climatology, there was used a comprehensive meteorological dataset was from Xavier et al. (2016). They used air temperature and rainfall data from meteorological stations to create an interpolated grid for all regions of Brazil. The grid has a 0.25º interval between each point and has information from 1980 to 2013 for air temperature, and from 1980 to 2015 for rainfall. For the present study, there were extracted information from unique nodes in the grid to represent four study sites, based on the latitude and longitude: A (Arambaré), TI (Tavares point I), TII (Tavares point II), and C (Central site) (Fig. 1). Then, a node located at -31.29, -051.0956 for rainfall information was selected. That one node was

inside a threshold of 0.50° encompassing all the four study sites above mentioned and offering the most complete time series dataset. Another node selected (-30.0500 and -051.1600) had a threshold of 1.5° encompassing those four study sites and corresponded to a larger time series of air temperature. Finally, the monthly accumulated rainfall and the monthly mean air temperature were calculated. Recent data of wind speed and direction (from July 2019 to June 2020) were also obtained from the same meteorological stations of Arambaré and Tavares towns for plotting 3-day, 5-day and daily wind rose diagrams. Daily river discharge data were obtained from ANA (National Water Agency - http://www2.ana.gov.br), from January 2016 to March 2020, for the Guaíba and Camaquã rivers, which are major contributors to the northernmost part of Patos Lagoon (Vaz et al., 2006). Then, there were also built graphs for this time interval for relating them to correspondent NDCI time series.

SATELLITE DATA DERIVED (RELATIVE) CHLOROPHYLL A INDEX, AND ITS RELATION WITH WATER TEMPERATURE

To relate with the chlorophyll-*a* biomass, the water temperature was retrieved from MODIS (Moderate Resolution Imaging Spectroradiometer) -Terra imagery as follows: Arambaré (-31.0349, -051.4253), Central site (-31.3189, -051.4725), Tavares point I (-31.1296, -051.2828), and Tavares point II (-31.3454, -051.2499). These temperature data were given as Land Surface Temperature (LST) and were subsequently transformed into the Celsius scale. Also, there was used the same time interval (July 2019 to June 2020) to obtain the phytoplankton biomass index known as Normalized Difference Chlorophyll-*a* Index (NDCI according to Mishra and Mishra, 2012), which is derived from Sentinel-2 images. NDCI is based on the use of the 708nm and 655nm

bands combined to evaluate bloom status in the water. When NDCI equaled to zero, it means that chlorophyll *a* biomass was approximately around 14 mg m^{-3} (Mishra and Mishra, 2012). NDCI values higher or lower than zero were not necessarily in linear regression with absolute chlorophyll *a* biomass value. However, NDCI>0 was associated with bloom conditions, and NDCI<0 did not mean lack of chlorophyll-a biomass. The calculated NDCI was adopted to relate with any spatial and temporal, environmental, and meteorological variability since there was no available *in-situ* chlorophyll-a dataset for the study area. To verify the association between the meteorological and climatological parameters and NDCI, the satellite data were interpolated to a daily interval.

RESULTS

DISTRIBUTION PATTERNS OF AUTOTROPHIC BIOMASS BASED ON NDCI IMAGERY

Typical blue-green cyanoHABs were registered by local citizens on Patos Lagoon (Fig.2) on December 30th, 2020, and January 13th, 2021. Some spatial and temporal distribution patterns of NDCI values for the main part of Patos Lagoon were seen in the same period. In December 2019, there were depicted high NDCI values throughout a few days up to 31st December, especially close to the east margin of Patos Lagoon (Fig. 3). Following this event, while the east margin kept with more patches of high NDCI, both NDCI and observational data detected a bloom event on the west margin on 13th January 2020), however, 10th January had the highest NDCI value for the region. It was estimated that high NDCI began on 3rd January and lasted for one week. High NDCI values were placed northwards, mainly near the east margin (Fig. 3). In general, there were also observed considerable NDCI patches in the other sites such as in the west and estuarine portion of PL.

Figure 2: Photographs of the bloom events: A: in Tavares, December 30th, 2019. B and C: in Arambaré, January 13th, 2020. Source: A. Local citizens, B. Clic Camaquã (available at www.cliccamaqua.com.br

METEOROLOGICAL AND HYDROLOGICAL FEATURES AND RELATION WITH NDCI VALUES

Rainfall and air temperature for the austral warmer period (November-December 2019 to January-February 2020) were compared with the monthly mean (± standard deviation) rainfall (Table 1) and air temperature (Table 2) for a climatology time series of *circa* thirty years (1980-2013), both for the west margin (Camaquã weather station) and east margin (Mostardas weather station) at the main part of Patos Lagoon (Fig. 1). A lower rainfall (<<80 mm, on average) than the monthly climatology mean was observed on both stations, except on January 2020. However, looking closer to the daily

rainfall rates on that month, both stations had higher precipitation precisely on January 10th (Fig. 4).

Table 1: Monthly 30-year average rainfall [in mm; from 1980–2015, according to Xavier et al. (2016)] and rainfall data obtained from the Camaquã's and Mostardas' meteorological stations, respectively, during 2019–2020. Note the values in black from November 2019 to February 2020 highlight our summer period studied with cyanobacterial blooms.

	30-year average rainfall (mm)		Camaquã's station (mm)		Mostardas' station (mm)	
Month	Mean	Standard deviation	2019	2020	2019	2020
January	76.5	52.2	139.2	**155.6**	83.6	**85.4**
February	88.1	49.0	70.8	**35.4**	50.4	**19.8**
March	90.9	59.0	81.2	44.8	-	27.4
April	98.9	62.3	78.6	48.2	-	28.6
May	115.5	69.1	278.4	117.6	-	0.00
June	123.1	65.4	41.2	165.2	47.6	25.2
July	137.8	80.4	179.8		137	
August	114.5	70.1	155		131	
September	133.8	65.1	108.8		103.8	
October	120.5	79.0	127.8		238.2	
November	80.6	56.4	**44.6**		**59.2**	
December	85.8	64.5	**76.6**		**19.2**	

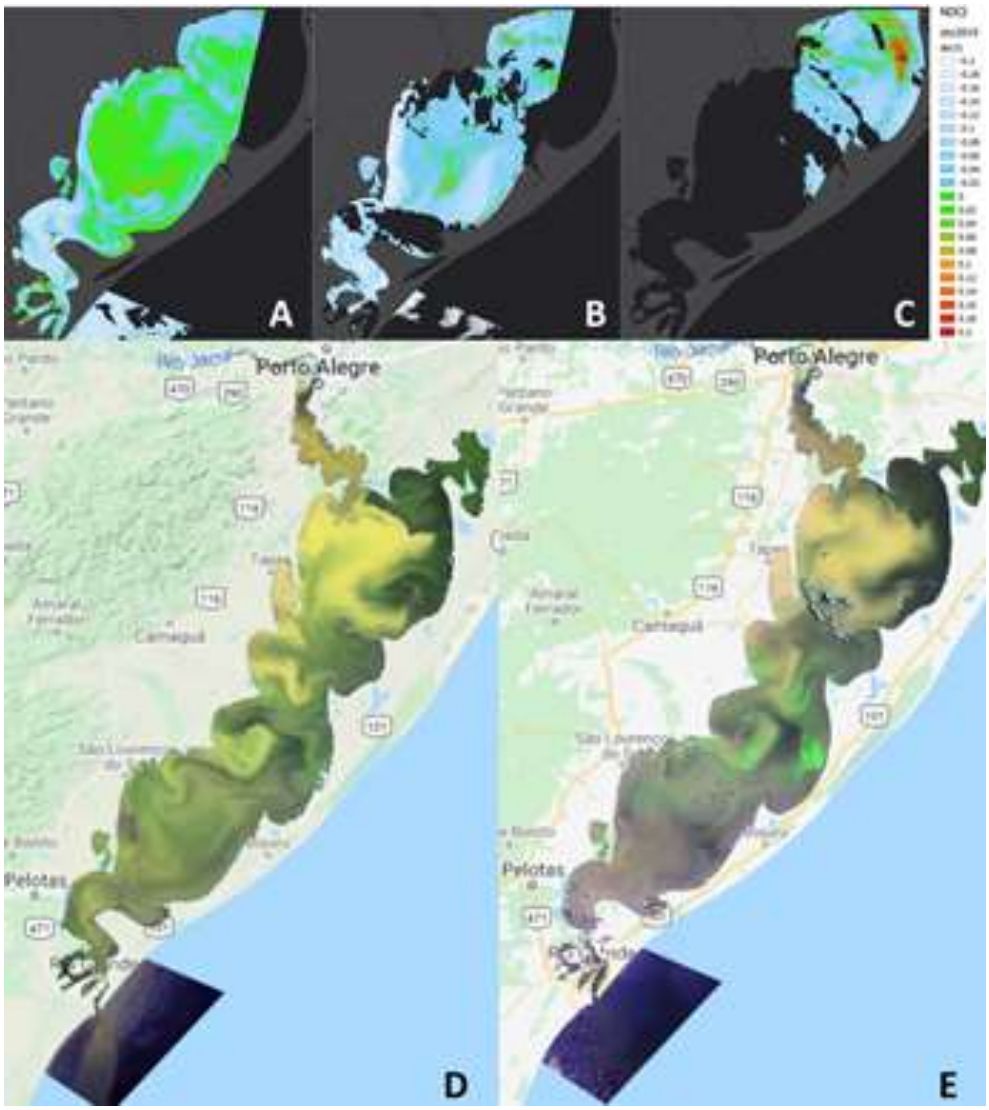

Figure 3: Images of Normalized Difference Chlorophyll-a Index (NDCI) derived from the Sentinel-2 data for the 2019 year: A –24th December, B –29th December, C –30th December (that latter one was a day before the first bloom event observed). Composite images for the whole Patos Lagoon on 5th January (D) and10th January (E) 2020, whose the latter day was of a second bloom photographed

There were slight differences in air temperature between both margins of PL. Low air temperatures were observed from November 2019 up to February 2020 in comparison with the climatology time series (Table 2), particularly in January 2020 (24.5°C). Regarding the local pattern in wind speed and direction (Fig. 5a-f), it was observed weak winds (<<6 m s^{-1}) on the bloom days (NDCI>>0) at both margins of Patos Lagoon (Fig. 5c-f), being weaker (<4 m s^{-1}) during January 2020 (Fig. 5f). Between three and five days before bloom events, strong NE winds (up to 12 m s^{-1}) were prevalent at the

east margin in December 2019, whereas at the west margin there was not a predominant wind direction in January 2020 (Fig. 5a-f). From July 2019 up to June 2020, our four sites chosen for describing the relation between water temperature and NDCI showed higher values only in January 2020, spanning from 0.1 to 0.2 of NDCI near the eastern margin. This month had a water temperature higher than 20ºC (Fig. 6a-d). Comparing the relation between river discharge and NDCI from January 2016 to March 2020, it was also noticeable high NDCI always in January each year, particularly in 2020 and 2018 when river discharge was lower than 2000 $m^3 s^{-1}$ (Fig. 7a-d).

Table 2: Monthly 30-year mean air temperature [in ºC; from 1980–2015, according to Xavier et al. (2016)] and air temperature data obtained from the Camaquã's and Mostardas' meteorological stations, respectively, during June 2019–July2020.

Month	**30-year mean air temperature (+-sd; ºC)**	**Camaquã's mean air temperature (+-sd; ºC) 2019**	**Camaqua's mean air temperature (+-sd; ºC) 2020**	**Mostardas' mean air temperature (+-sd; ºC) 2019**	**Mostardas' mean air temperature (+-sd; ºC) 2020**
January	25.56 (5.74)	24.84 (4.27)	23.42 (3.97)	25.90 (2.88)	24.50 (2.44)
February	25.47 (5.56)	23.00 (4.28)	23.05 (4.60)	25.63 (2.54)	23.54 (2.77)
March	24.39 (5.65)	21.40 (4.35)	23.03 (4.42)	26.84 (2.31)	23.76 (1.09)
April	21.26 (5.88)	19.96 (3.75)	18.88 (4.26)	-	20.34 (2.67)
May	17.95 (5.90)	17.47 (3.19)	15.64 (4.73)	-	16.86 (3.47)
June	15.29 (6.14)	16.93 (4.42)	14.77 (4.75)	16.99 (4.51)	15.55 (2.69)
July	14.67 (6.44)	12.24 (4.91)	-	13.24 (3.70)	-
August	16.39 (6.82)	13.71 (5.30)	-	14.30 (3.53)	-
September	17.46 (6.13)	15.05 (4.78)	-	15.51 (2.67)	-
October	20.23 (6.03)	19.26 (5.02)	-	18.75 (2.41)	-
November	22.27 (6.14)	21.30 (4.29)	-	20.98 (2.04)	-
December	24.35 (6.14)	22.98 (5.56)	-	22.58 (3.09)	-

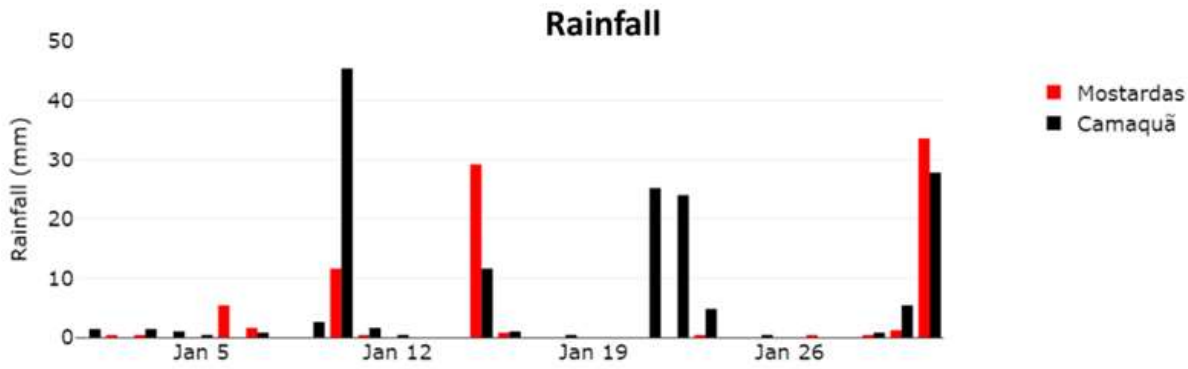

Figure 4: Daily rainfall from the Camaquã's (black) and Mostardas' (red) meteorological stations during January 2020.

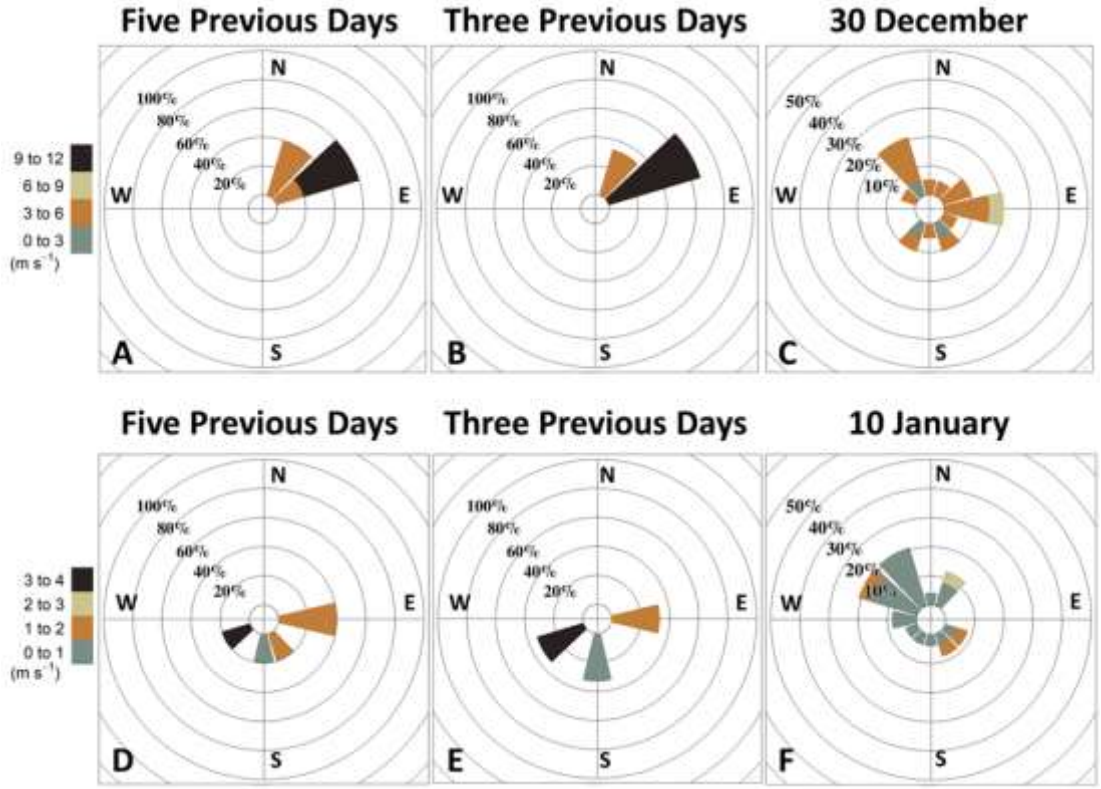

Figure 5: Upper panel: Wind speed and direction from the Mostardas' meteorological station for five days before (A), three days before (B), and on the day 30th December (C) of bloom. Lower panel: Wind speed and direction from the Camaquã's meteorological station for five days before (A), three days before (B), and on the day 10th January (C) of bloom

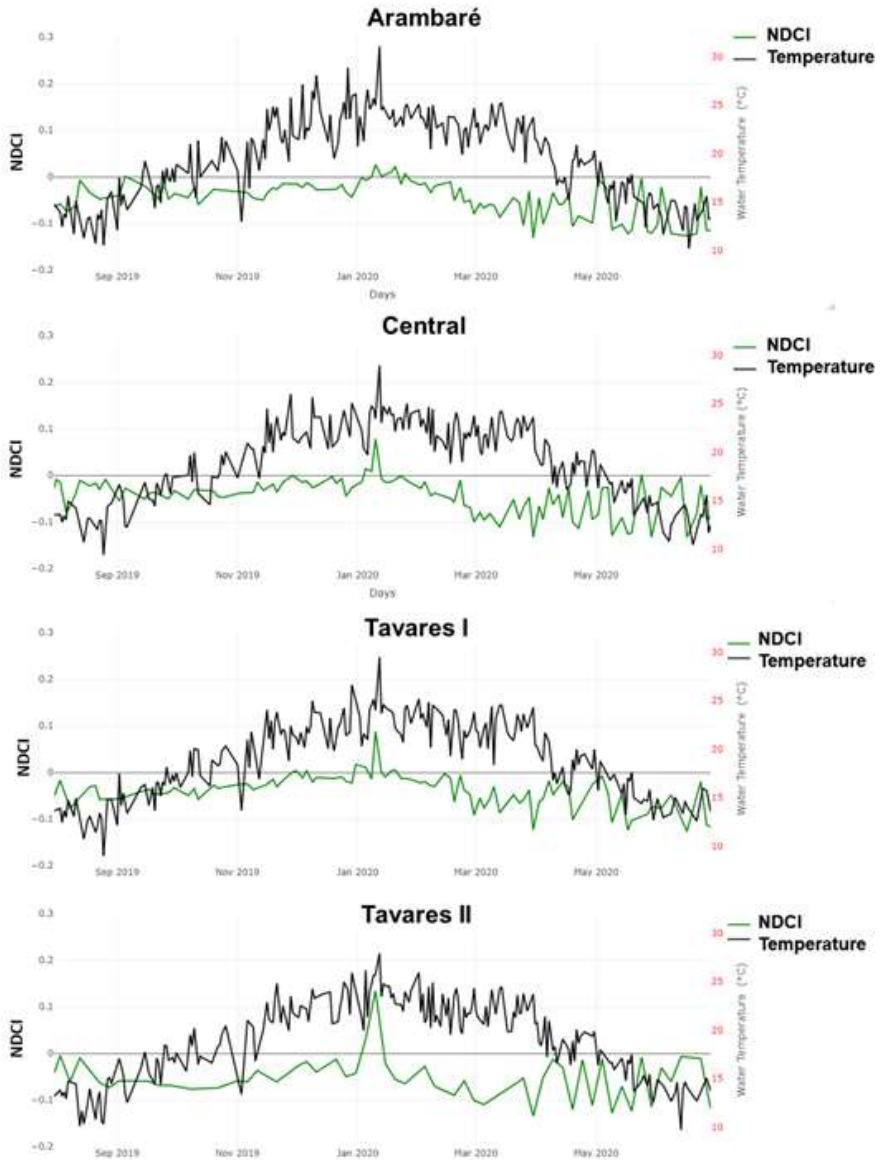

Figure 6: NDCI (green lines) and water temperature (black lines) from August 2019 to June 2020, for the study sites of Arambaré, Center, Tavares I and Tavares II, respectively. Note NDCI was derived from the Sentinel-2 data, and water temperature was retrieved from the MODIS-Aqua

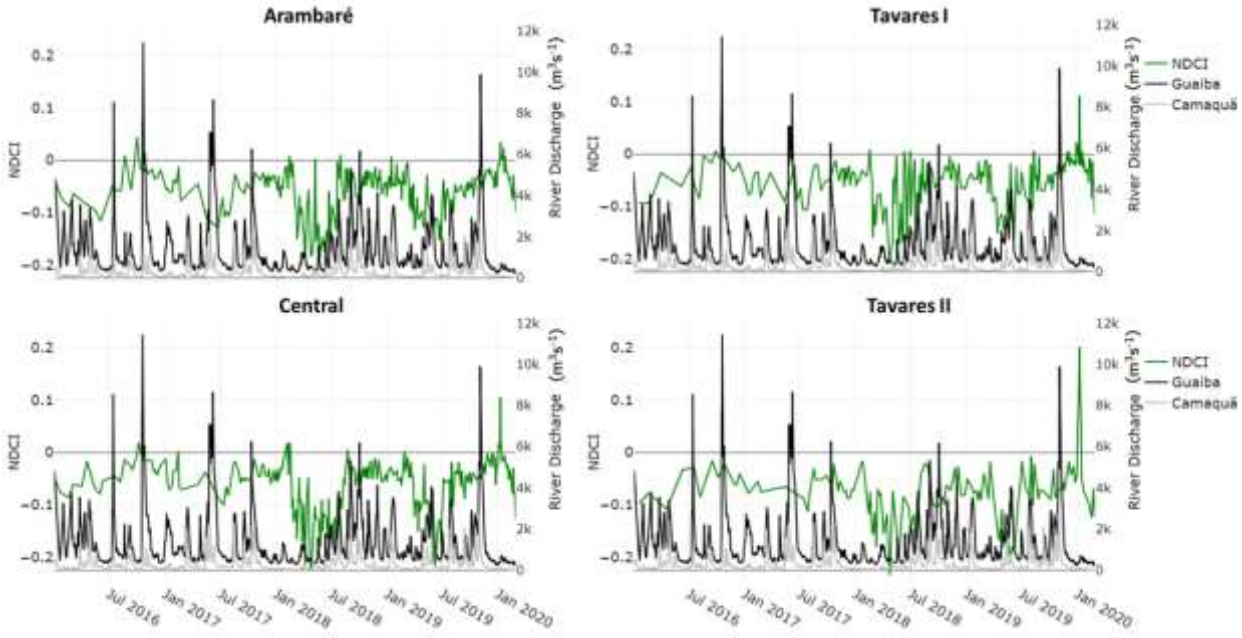

Figure 7: Time series of NDCI (green lines) for the study sites of Arambaré, Center, Tavares I and Tavares II, respectively, and river discharge data series of Guaíba (black lines) and Camaquã (gray lines) from January 2015 to March 2020

DISCUSSION

CYANOHABS ACROSS PATOS LAGOON UNDER THE INFLUENCE OF EXTREME METEOROLOGICAL EVENTS

Results described biological features based on NDCI during mainly the austral warmer period (of 2019–2020) when cyanobacteria such as *Microcystis* spp. and *Dolichospermum* spp. tend to be prominent within the Patos Lagoon system (Ferreira et al., 2004; Odebrecht et al., 2005; Yunes, 2009; Odebrecht et al., 2010; Hariguchi et al., 2015;). Differently from all these works that concentrated along the estuarine part of PL, the idea behind this work was to relate the NDCI distribution patterns with the meteorological and climatic forces in the large limnic part of that lagoon.

Several works demonstrated concern about the high frequency and magnitude of cyanoHABs in freshwater systems linked to cultural eutrophication (Carpenter et al.,

1998; Reynolds and Davies, 2001) and climate change scenarios (Paerl and Huisman, 2009; Kennish and Paerl, 2010 and references therein; Reichwaldt and Ghadouani, 2012; Paerl and Otten, 2013). Besides these, other studies highlighted the threats of cyanoHABs to the ecosystem and social and economic activities (de Souza et al., 2018; Paerl et al., 2015; Paerl, 2017). However, no nutrient dataset was available to seek a sign of cultural eutrophication over the NDCI distribution patterns during the studied period. Even so, results demonstrated that the summer of 2019–2020 was particularly drier than the climatological mean (Xavier et al., 2016) for the Patos Lagoon region. Low rainfall and river discharge is expected to be reflected in the high retention time of waters. Coupled with high temperatures and thermal stratification in summer, these conditions all together might have promoted cyanobacteria growth and accumulations across the main part of PL. NDCI values higher than zero were also seen at the estuarine part of PL, which can be indicative of the presence of cyanobacteria as it was observed *in situ* samples in other summer periods (Yunes et al., 1998; Ferreira et al., 2004; Fujita and Odebrecht, 2007; Haraguchi et al., 2015).

DIFFERENCES BETWEEN THE MARGINS OF PATOS LAGOON AND METEOROLOGICAL VARIABILITY

Concerning the influence of wind patterns on the cyanobacteria dynamics, results indicated moderate (3.86 ms^{-1}) to weak (0.70 ms^{-1}) winds in the east and west part of PL, respectively, in those days of higher NDCI values. On the other hand, three to five days before those high primary producers' biomass, the main part of Patos Lagoon was under strong winds of up to 8.09 ms^{-1}. We suggest that under those strong winds there was the water column mixing and advection of biomass across the whole water body. As the high hourly and daily wind variability is commonplace, there were observed that reducing wind speed to 1.71–2.04 ms^{-1} and lower would be necessary for the surface

accumulation of primary producers' biomass across many places of the Patos Lagoon system. A similar pattern can be observed in Lake Winnipeg, where calm winds allow the cyanobacteria accumulation after strong winds mixing events (Binding et al., 2018). The five days before the Arambaré's bloom event was characterized by strong winds from the 3rd quadrant and an average speed of 1.71 ms^{-1}; when analyzed only the three previous days there was an increase in the average speed (1.71 to 2.04 ms^{-1}) and frequency of the SW winds. On the other hand, the five days before the Tavares' bloom event had a NE wind predominance with high speed (6.70 ms^{-1}) that was kept up to three previous days, with even higher speed (8.09 ms^{-1}).

The average rainfall for the period (November to February) for the past thirty years was 331.1 mm, while for 2019/2020 summer the average was lower for both *in situ* meteorological stations (Camaquã and Mostardas). An exception was seen for Camaquã rainfall in January 2020 (155.6 mm), otherwise, the remaining months showed lower rainfall values than the average. On the other hand, Mostardas' values were almost half average rainfall for the period (183.6 mm compared with 331.1 mm). In this way, the two bloom events were observed before the relatively high rainfall rates in January 2020. Then, it would be possible that the NDCI-indicated bloom had been affected by the high precipitation, which was measured after 6 PM (see Fig. 4).

The days before the highest NDCI observed in 10th January bloom (03rd, 05th, and 08th Jan) also showed large blooms but with smaller intensity, according to the NDCI color scale (see Fig. 3). Due to the Sentinel-2 passage periodicity, it was not possible to analyze 30th December, so the next 31st December was inspected. This latter day NDCI was higher near the east margin, and a small patch was seen at the west margin. Likewise, there was possible to observe smaller, but more extended NDCI values on the previous days (19, 24, 29 December; Fig. 3a-c).

CONCLUSION

For the 2019/2020 summer, two cyanobacterial bloom events were registered within the limnic area of PL. That summer period was drier compared to climatological data, which may have affected the residence time and allowed the development and accumulation of such blooms. These blooms were fairly represented with the Normalized Difference Chlorophyll *a* Index, showing that this tool can be considered for monitoring and management of cyanoHABs in southern Brazilian waterbodies.

We suggested that river discharge (and flow rates) influence over blooms dynamics would be associated with the residence time in the limnic part of PL. However, further studies should focus on the export rate and the time delay between the river discharge and advection of the cyanobacterial biomass.

The wind force should have a more complex influence on the cyanoHAB dynamics since it would be related to the cyanobacteria transport across the lagoon and it would be also coupled with water mixing and resuspension of cyanobacterial populations. This kind of study can be accomplished in further work with a 3D hydrodynamical model, which can represent the vertical mixing missed in this present work. Nonetheless, it seemed that weak winds were responsible for the accumulation of cyanobacterial biomass at the central parts of PL. This accumulation process can be an ecological and economic threat to human populations inhabiting around those Patos Lagoon margins.

ACKNOWLEDGMENTS

The authors thank two anonymous people for sending their photographs of the accumulation of cyanobacteria at the Patos Lagoon's margins, in the summer of 2019–2020. B.F. Canever is granted an MSc fellowship (CAPES) number 88887.342873/2019-00. M.S. de Souza is granted a PNPD/MEC-CAPES fellowship number 88882.314596/2019-01. The authors declare no conflict of interest. At last, but not least, this work was endorsed by the GlobalHAB/IOC-SCOR.

AUTHOR CONTRIBUTION

B.F.C.: Conceptualization; Formal Analysis; Investigation; Writing - original draft; Writing – review & editing;

M.S.S.: Conceptualization; Writing - original draft; Writing – review & editing;

E.V.K.: Methodology; Meteorological Data; Writing – review & editing;

F.L.L..: Methodology; Remote Sensing Data; Writing – review & editing;

E.H.L.F..: Supervision; Writing – review & editing;

J.S.Y.: Supervision; Project Administration; Writing – review & editing;

REFERENCES

AGUILERA, L., SANTOS, A.L.F. ROSMAN, C.P.C., 2020. On characteristic hydraulic times through hydrodynamic modeling: discussion and application in Patos Lagoon (RS). *Revista Ambiente & Água.* 15.

BINDING, C.E., GREENBERG, T.A., MCCULLOUGH, G., WATSON, S.B., PAGE, E., 2018. An analysis of satellite-derived chlorophyll and algal bloom indices on Lake Winnipeg. *Jounarl of Great Lakes Research* 44, 436–446.

BITENCOURT, L. P., FERNANDES, E. H., DA SILVA, P. D., & MÖLLER JR, O.,2020. Spatio-temporal variability of suspended sediment concentrations in a shallow and turbid lagoon. *Journal of Marine Systems*, *212*, 103454.

BORTOLIN, E.C., WESCHENFELDER, J., FERNANDES, E.H., BITENCOURT, L.P., MÖLLER, O.O., GARCÍA-RODRÍGUEZ, F., TOLDO, E., 2020. Reviewing sedimentological and hydrodynamic data of large shallow coastal lagoons for defining mud depocenters as environmental monitoring sites. *Sedimentary Geology* 410, 105782.

CARPENTER, S. R., CARACO, N. F., CORRELL, D. L., HOWARTH, R. W., SHARPLEY, A. N., & SMITH, V. H.,1998. Nonpoint pollution of surface waters with phosphorus and nitrogen. *Ecological Applications*, *8*(3), 559-568.

CLOERN, J.E., 2001. Our evolving conceptual model of the coastal eutrophication problem. *Marine Ecology Progress Series*. 210, 223–253.

DE SOUZA, M.S., MUELBERT, J.H., COSTA, L.D.F., KLERING, E. V., YUNES, J.S., 2018. Environmental Variability and Cyanobacterial Blooms in a Subtropical Coastal Lagoon: Searching for a Sign of Climate Change Effects. *Frontiers in Microbiology* 9, 1–12.

FERNANDES, E. H. L., DYER, K. R., MOLLER, O. O., & NIENCHESKI, L. F. H., 2002. The Patos lagoon hydrodynamics during an El Nino event (1998). *Continental Shelf Research*, 22(11-13), 1699-1713.

FERREIRA, A., MINILLO, A., SILVA, L., YUNES, J., 2004. Ocorrência de Anabaena spiroides (cianobactéria) no estuário da Lagoa dos Patos (RS, Brasil) no verão-outono de 1998. *Atlântica (Rio Grande)* 26, 17–26.

FUJITA, C.C., ODEBRECHT, C., 2007. Short-term variability of chlorophyll a and phytoplankton composition in a shallow area of the Patos Lagoon estuary (Southern Brazil). *Atlântica* (*Rio Grande)* 29, 93–106.

HARAGUCHI, L., CARSTENSEN, J., ABREU, P.C., ODEBRECHT, C., 2015. Long-term changes of the phytoplankton community and biomass in the subtropical shallow Patos Lagoon Estuary, Brazil. *Estuarine, Coastal and Shelf Science* 162, 76–87.

HO, J.C., MICHALAK, A.M., 2017. Phytoplankton blooms in Lake Erie impacted by both long-term and springtime phosphorus loading. *Journal of Great Lakes Research* 43, 221–228.

IPCC, 2021: Climate Change 2021: The Physical Science Basis. Contribution of Working Group I to the Sixth Assessment Report of the Intergovernmental Panel on Climate Change [Masson-Delmotte, V., P. Zhai, A. Pirani, S.L. Connors, C. Péan, S. Berger, N. Caud, Y. Chen, L. Goldfarb, M.I. Gomis, M. Huang, K. Leitzell, E. Lonnoy, J.B.R. Matthews, T.K. Maycock, T. Waterfield, O. Yelekçi, R. Yu, and B. Zhou (eds.)]. Cambridge University Press. In Press.

KALIKOSKI, D.C., VASCONCELLOS, M., 2012. Case study of the technical, socio-economic and environmental conditions of small-scale fisheries in the estuary of Patos Lagoon, Brazil: a methodology for assessment, FAO fisheries and aquaculture circular.

KENNISH, M.J., PAERL, H.W., 2010. Coastal lagoons: critical habitats of environmental change, in: CRC Press.

KING, K.W., WILLIAMS, M.R., FAUSEY, N.R., 2015. Contributions of Systematic Tile Drainage to Watershed-Scale Phosphorus Transport. *Journal of Environmental Quality* 44, 486–494.

KJERFVE, B., 1994. Coastal lagoons. In *Elsevier oceanography series* (Vol. 60, pp. 1-8). Elsevier.

LEHMAN, P.W., BOYER, G., HALL, C., WALLER, S., GEHRTS, K., 2005. Distribution and toxicity of a new colonial Microcystis aeruginosa bloom in the San Francisco Bay Estuary, California. Hydrobiologia 541, 87–99.

LOBO, F. DE L., NAGEL, G.W., MACIEL, D.A., DE CARVALHO, L.A.S., MARTINS, V.S., BARBOSA, C.C.F., DE MORAES NOVO, E.M.L., 2021. Algaemap: Algae bloom monitoring application for inland waters in Latin America. *Remote Sensing* 13.

MARQUES, W.C., 2012. The Temporal Variability of the Freshwater Discharge and Water Levels at the Patos Lagoon, Brazil. *International Journal of Geosciences*. 03, 758–766.

MENDES, C.R.B., ODEBRECHT, C., TAVANO, V.M., ABREU, P.C., 2017. Pigment-based chemotaxonomy of phytoplankton in the Patos Lagoon estuary (Brazil) and adjacent coast. *Marine Biology Research* 13, 22–35.

MICHALAK, A.M., ANDERSON, E.J., BELETSKY, D., BOLAND, S., BOSCH, N.S., BRIDGEMAN, T.B., CHAFFIN, J.D., CHO, K., CONFESOR, R., DALOGLU, I., DEPINTO, J. V., EVANS, M.A., FAHNENSTIEL, G.L., HE, L., HO, J.C., JENKINS, L., JOHENGEN, T.H., KUO, K.C., LAPORTE, E., LIU, X., MCWILLIAMS, M.R., MOORE, M.R., POSSELT, D.J., RICHARDS, R.P., SCAVIA, D., STEINER, A.L., VERHAMME, E., WRIGHT, D.M., ZAGORSKI, M.A., 2013. Record-setting algal bloom in Lake Erie caused by agricultural and meteorological trends consistent with expected future conditions. *Proceedings of the National Academy of Sciences of the United States of America* 110, 6448–6452.

MISHRA, S., MISHRA, D.R., 2012. Normalized difference chlorophyll index: A novel model for remote estimation of chlorophyll-a concentration in turbid productive waters. *Remote Sensing of Environment*. 117, 394–406.

MISHRA, S., STUMPF, R.P., SCHAEFFER, B.A., WERDELL, P.J., LOFTIN, K.A., MEREDITH, A., 2019. Measurement of Cyanobacterial Bloom Magnitude using Satellite Remote Sensing. *Scientific reports* 9, 1–17.

MÖLLER, O. O., & CASTAING, P.,1999. Hydrographical characteristics of the estuarine area of Patos Lagoon (30 S, Brazil). In *Estuaries of South America* (pp. 83-100). Springer, Berlin, Heidelberg.

MOLLER, O.O., CASTAING, P., SALOMON, J.C., LAZURE, P., 2001. The influence of local and non-local forcing effects on the subtidal circulation of Patos Lagoon. *Estuaries* 24, 297–311.

MÖLLER, O.O., CASTELLO, J.P., VAZ, A.C., 2009. The effect of river discharge and winds on the interannual variability of the pink shrimp Farfantepenaeus paulensis production in Patos Lagoon. *Estuaries and Coasts* 32, 787–796.

ODEBRECHT, C., ABREU, P.C., BEMVENUTI, C.E., COPERTINO, M., MUELBERT, J.H., VIEIRA, J.P., AND SEELIGER, U., 2010. The Patos Lagoon estuary: Biotic responses to natural and anthropogenic impacts in the last decades (1979–2008). *In:* Kennish, M.J. and Paerl, H.W. (eds.). *Coastal Lagoons: Critical habitats of environmental change.* Chapter 17, pp: 437–459. *CRC Marine Science Series, CRC Press,* Boca Raton.

ODEBRECHT, C., SELLIGER, U., COUTINHO, R., AND TORGAN, L.C. (1987). "Florações de Microcystis (cianobactérias) na Lagoa dos Patos, RS," in *Proceedings of the 1st Simpósio sobre Ecossistemas Costeiros Sul e Sudeste do Brasil: Síntese do Conhecimento,* ed ACIESP (Águas de Lindóia: ACIESP), 11–16.

ODEBRECHT, C., ABREU, P. C., MÖLLER, O. O., NIENCHESKI, L. F., PROENÇA, L. A., & TORGAN, L. C.,2005. Drought effects on pelagic properties in the shallow and turbid Patos Lagoon, Brazil. *Estuaries*, *28*(5), 675-685.

PAERL, H.W., 2017. Controlling harmful cyanobacterial blooms in a climatically more extreme world: Management options and research needs. *Journal of Plankton Research* 39, 763–771.

PAERL, H.W., HUISMAN, J., 2009. Climate change: A catalyst for global expansion of harmful cyanobacterial blooms. *Environmental Microbiology Reports*. 1, 27–37.

PAERL, H.W., OTTEN, T.G., 2013. Harmful Cyanobacterial Blooms: Causes, Consequences, and Controls. *Microbial Ecology* 65, 995–1010.

PAERL, H. W., YIN, K., & O'BRIEN, T. D.,2015. SCOR Working Group 137:" Global Patterns of Phytoplankton Dynamics in Coastal Ecosystems": An introduction to the special issue of Estuarine, Coastal and Shelf Science. *Estuarine Coastal and Shelf Science*, *162*, 1-3.

PAERL, H.W., GARDNER, W.S., HAVENS, K.E., JOYNER, A.R., MCCARTHY, M.J., NEWELL, S.E., QIN, B., SCOTT, J.T., 2016. Mitigating cyanobacterial harmful algal blooms in aquatic ecosystems impacted by climate change and anthropogenic nutrients. *Harmful Algae* 54, 213–222.

REICHWALDT, E. S., & GHADOUANI, A. ,2012. Effects of rainfall patterns on toxic cyanobacterial blooms in a changing climate: between simplistic scenarios and complex dynamics. *Water research*, *46*(5), 1372-1393.

REYNOLDS, C.S., AND DAVIES, P.S. (2001) Sources of bioavailability of phosphorus fractions in freshwaters: a British perspective. *Biological Reviews* **76**, 27–64.

TÁVORA, J., FERNANDES, E.H., BITENCOURT, L.P., OROZCO, P.M.S., 2020. El-Niño Southern Oscillation (ENSO) effects on the variability of Patos Lagoon Suspended Particulate Matter. *Regional Studies in Marine Science* 40, 101495.

THOMPSON, P. A., O'BRIEN, T. D., PAERL, H. W., PEIERLS, B. L., HARRISON, P. J., & ROBB, M. (2015). Precipitation as a driver of phytoplankton ecology in coastal waters: a climatic perspective. *Estuarine, Coastal and Shelf Science 162*, 119-129.

VAZ, A.C., MÖLLER JR, O.O., DE ALMEIDA., T.L., 2006. Análise quantitativa da descarga dos rios afluentes da Lagoa dos Patos. *Atlântica* (*Rio Grande)* 28, 13–23.

XAVIER, A.C., KING, C.W., SCANLON, B.R., 2016. Daily gridded meteorological variables in Brazil (1980–2013). *International Journal of Climatology* 36, 2644–2659.

YUNES, J.S., 2009. Florações de microcystis na lagoa dos patos e o seu estuário: 20 Anos de Estudos. *Oecologia Brasiliensis*. 13, 313–318.

YUNES, J.S., NIENCHESKI, L.F.H., SALOMON, P.S., PARISE, M., BEATTIE, K.A., RAGGETT, S.L., CODD, G.A., 1998. Effect of nutrient balance and physical factors on blooms of toxic cyanobacteria in the Patos Lagoon, southern Brazil. *Internationale Vereinigung für theoretische und angewandte Limnologie: Verhandlungen* 0770, 1796–1800.

Capítulo VI: Resultados e Discussão: Manuscrito 2

O segundo manuscrito, de autoria de Beatriz Feltrin Canever, Pablo Dias da Silva, Marcio Silva de Souza, Elisa Helena Leão Fernandes e João Sarkis Yunes é intitulado: "**ENSO effects on the summer transport and accumulation of cyanobacteria biomass in a large coastal lagoon (Patos Lagoon, southern Brazil)**" e foi submetido para publicação no periódico "Journal of Marine Systems".

ENSO effects on the summer transport and accumulation of cyanobacteria biomass in a large coastal lagoon (Patos Lagoon, southern Brazil)

Beatriz Feltrin Canever[1,4], Pablo Dias da Silva[2], Marcio Silva de Souza[3], Elisa Helena Leão Fernandes[2], João Sarkis Yunes[3]

[1] Programa de Pós-Graduação em Oceanologia – FURG – Rio Grande – RS - Brazil.

[2] Laboratório de Oceanografia Costeira e Estuarina – IO-FURG – Rio Grande – RS- Brazil

[3] Laboratório de Cianobactérias e Ficotoxinas – IO-FURG – Rio Grande – RS- Brazil

[4] Corresponding author: beatriz.canever@gmail.com
Present address:

Laboratório de Cianobactérias e Ficotoxinas

Instituto de Oceanografia - IO

Univ. Federal do Rio Grande - FURG

Av. Itália, Km 8, Carreiros PO Box 474, Rio Grande-RS-Brazil, 96203-270

Key Words: Harmful Algal Blooms, ENSO, wind-driven circulation, TELEMAC 3D, Patos Lagoon.

Abstract

Harmful blooms of *Microcystis* spp. have been studied in Patos Lagoon since the 1980s. The majority of these studies, however, explore its biological and biochemical characteristics, and none of them investigated the transport and accumulation of cyanobacteria colonies through the very large, limnic region of the Patos Lagoon. Wind and river discharge dominate the hydrodynamics of Patos Lagoon and have an interannual variability in phase with El Niño Southern Oscillation (ENSO). To calculate the exportation and accumulation of *Microcystis* spp. colonies the hydrodynamic and Lagrangian model TELEMAC 3D was used to analyze nine austral summers, from 2008 to 2017. Simulations periods were related with the ENSO (classification based on the Oceanic Niño Index - NOAA) cycles and with wind and river discharge data. Results showed that El Niño summers presented higher *Microcystis* spp. export due to positive rainfall anomalies. La Niña and Neutral Condition summers, on the other hand, were more susceptible to *Microcystis* spp. accumulation inside the lagoon.. Results presented are the first step forward towards

establishing cyanobacterial monitoring efforts on the most vulnerable places of Patos Lagoon to eutrophication processes and high densities of harmful cyanobacteria species.

1. Introduction

Harmful Algal Blooms (HABs) and their negative impact on biodiversity are widely distributed around the world (Hallegraeff et al., 2021), and their distribution and magnitude are expected to enhance climate change scenarios (Paerl et al., 2011, O'Neil et al., 2012). However, field-based monitoring of these blooms demands high human, financial and temporal resources. For this reason, indirect methods are being tested to investigate such events with low cost, expecting to facilitate the monitoring and management of the problem (Wynne et al., 2011, Aleynik et al., 2016; Soontiens et al., 2019).

Numerical modeling techniques proved to be a useful tool to calculate the transport of different HABs, being able to assess the effects of wind, currents, and tides upon the bloom dynamics (Aleynik et al., 2016; Havens et al., 2010; Qin and Lin, 2019). Due to the buoyant characteristic of phytoplankton, Lagrangian models can be used to understand this blooms' dynamic focusing only on the advection of the colonies, without considering biological factors such as growth and nutrient intake (Wynne et al., 2011).

Cyanobacterial HABs have been recorded in Patos Lagoon since 1980 (Odebrecht et al., 1987), although according to local inhabitants the blooms occurred since the beginning of the XX Century (Yunes, 2009). HABs offer risk to the population living at the margins of Patos Lagoon and to tourists who go there to enjoy summer. These places also gather several fishing villages that rely on fish and shrimp for their sustenance. Part of the population living near the lagoon depends on its waters for agriculture, and at least two cities for drinking purposes and other economic uses. Adjacent to Patos Lagoon there is Cassino beach by the ocean coast, known as a popular place, chosen by tourists during summer. Undocumented complaints of allergies caused by cyanobacteria toxins were recorded on the beach in 2003, with no further studies on the subject (Silva, 2005). Yunes et al. (1996) and Yunes (2009) reported that HABs tend to happen throughout Patos Lagoon every summer.

Like any other plankton population, Cyanobacterial HABs distribution and transport respond to water circulation, in other words, to the wind (Liu et al., 2019; Wu et al., 2010) and freshwater discharges (Kruk et al., 2021). As a microtidal system, Patos Lagoon hydrodynamics is highly influenced by both driving forces (Möller et al., 2001). Bitencourt et al. (2020a) and Távora et al. (2020) explained that the El Niño Southern Oscillation (ENSO) cycles play an important role in the lagoon circulation in an interannual time scale. The effects of ENSO in southern South America are well documented: during the El Niño (warm) events, the precipitation anomaly is positive while during La Niña (cold) events the precipitation anomaly is negative (Grimm et al., 1998). Anomalies in precipitation result in anomalies in freshwater, increasing (decreasing) the seaward flow during El Niño (La Niña) periods (Barros and Marques, 2012; Fernandes et al., 2002). Bitencourt et al. (2020a) and Távora et al. (2020) have demonstrated that ENSO cycles also affect the wind stress over the Lagoon, and although both events have a predominance of northern winds, La Niña events have a higher frequency of SW winds in comparison with El Niño. The ENSO influence in Patos Lagoon also affects the local biota with results depending on the El Niño intensity, with strong events enhancing the biodiversity of fishes (Possamai et al., 2018), decreasing species abundance (Belarmino et al., 2021), and dropping growth rates (Reis-Santos et al., 2021). The impact of ENSO on the phytoplankton community, including cyanobacteria, has been investigated in Latin America (Devercelli, 2010; Solari et al., 2014). However, for the Patos Lagoon, there are few kinds of this study, being the majority of works limited to the estuary (Vieira et al., 2008; They et al., 2015), and even some studies related to phytoplankton community ecology (Odebrecht et al., 2015).

Thus, the present study aims to understand how the ENSO cycles affect the *Microcystis* spp. distribution inside the Patos Lagoon and its export towards the ocean.

1.1 Study area

Patos Lagoon is located between 30º12'–32º12'S, 50º40'–52º15'W (Fig. 1) and is considered the largest choked coastal lagoon in the world (Kjerfve, 1986). The lagoon's only connection with the ocean is through a 700 m wide channel (Moller et al., 2001; Bitencourt et al., 2020b), which attenuates the tides acting as a filter (Fernandes et al., 2004; Moller et al., 1996). Due to this reduced tidal influence, the main physical forcing

on the lagoon are the freshwater discharges and local and non-local wind (Möller et al., 2001). Non-local wind effects on circulation are concentrated in the estuarine region, where local wind stress and river flow determine the circulation inside the lagoon (Möller et al., 2001).

The three main tributaries of the Patos Lagoon are Guaíba and Camaquã rivers, and São Gonçalo channel, with a total mean annual freshwater discharge of 2400 m^3s^{-1} (Vaz et al., 2006). The river flow modulates the ebb conditions on the south connection with the ocean (Marques et al., 2009), and when the river discharge reaches above 2000 m^3s^{-1} the wind influence on the hydrodynamics is overshadowed by the river flow (Möller and Castaing, 1999). The Patos Lagoon hydrodynamics is also influenced by interannual variability related to ENSO cycles, affecting mostly the river discharges (Barros and Marques, 2012). El Niño events intensify the freshwater discharge into the lagoon, consequently enhancing the flow towards the ocean, and in extreme episodes preventing the saltwater intrusion inside the lagoon (Fernandes et al., 2002; Barros and Marques, 2012; Bitencourt et al., 2020a). La Niña events have the opposite effect on the lagoon, with the reduced freshwater flow, facilitating salt intrusion landward (Barros and Marques, 2012; Bitencourt et al., 2020a,b).

The wind pattern over the Patos Lagoon region is dominated by NE winds, however, SW has higher intensity and occurs notably in austral winter associated with the passage of frontal systems over the area (Moller et al., 1996; Möller et al., 2001). Bitencourt et al., (2020b), observed that SW (NE) winds tend to increase (inhibit) saltwater intrusion into the lagoon and that NE (SW) winds tend to accumulate suspended sediment on the western (eastern) margin of the lagoon.

Microcystis is a potentially harmful cyanobacteria genus present in Patos Lagoon (Matthiensen et al., 2000, Yunes et al., 1996), which can synthesize microcystins and dermatoxins. This genus grows at temperatures higher than 20ºC (Yunes et al., 1996) and usually spends the austral summer on the water surface (Reynolds et al., 1981), having its motion controlled by the water dynamics. It is also during austral summer that the lagoon's environmental conditions are beneficial for *Microcystis*' growth (Matthiensen et al., 1999). Besides, the Patos Lagoon residence time during austral summer (dry season) is higher than during winter (wet season) (Aguilera et al., 2020).

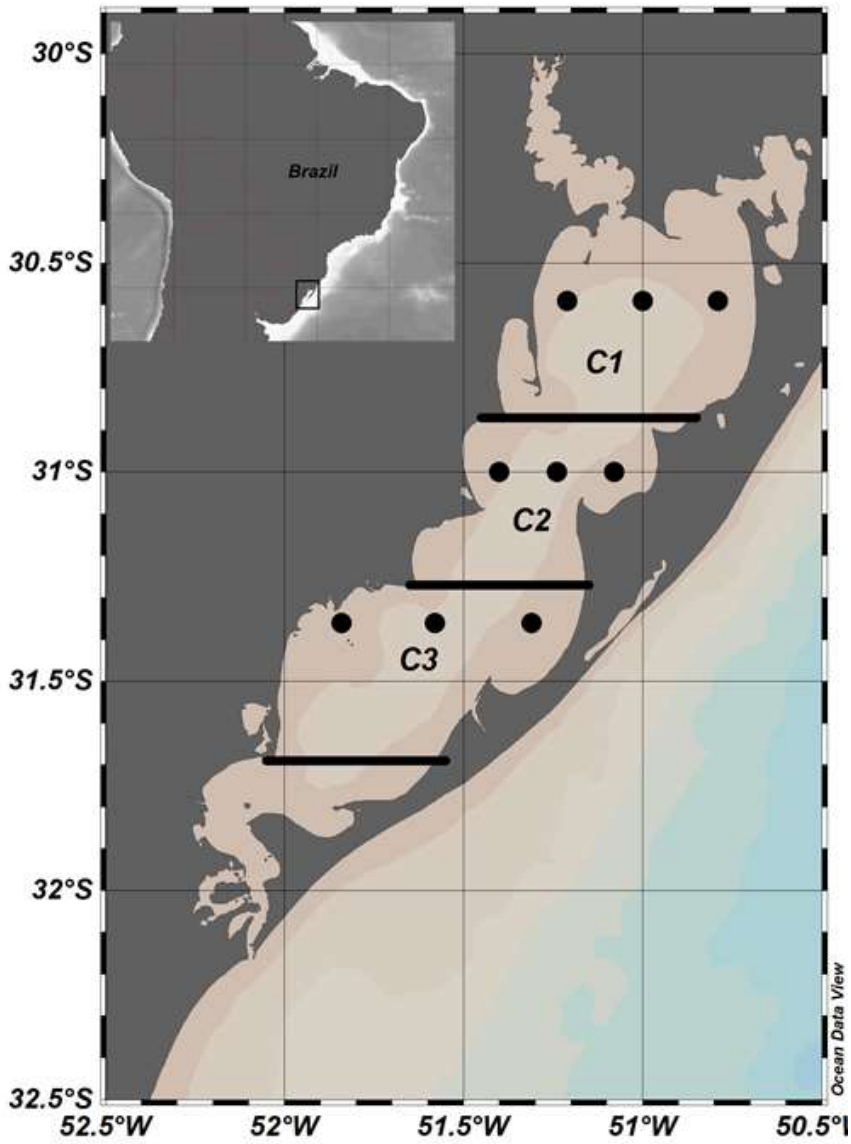

Figure 1: Inset map: Location of the Patos Lagoon in southern Brazil. Main map: Depiction of the three cells (C1, C2, and C3) within the Patos Lagoon, wherein black dots in each cell correspond to the initial position of the drogues. Those drogues were equally distributed across the cells in the numerical simulation.

2 Material and methods

2.1 Hydrodynamic model

In this study, hydrodynamic simulations were performed using the TELEMAC-3D model (http://www.opentelemac.org), to simulate the three-dimensional hydrodynamics of the Patos Lagoon. The model solves the Reynolds-averaged Navier-Stokes equations

and considers the local variations in the free surface of the fluid, neglecting the variation of density in the mass conservation equation, offering the choice of considering the hydrostatic or non-hydrostatic pressure and applying the Boussinesq approximation to solve the motion equation. Simulations were carried out in the hydrostatic mode. Details of the model formulations were presented by Hervouet (2007).

The model applies the finite element method to solve the hydrodynamic equations and uses the sigma coordinate system for vertical discretization. Its domain was discretized by a non-structured grid of finite elements (triangular elements), which allowed the concentration of a higher number of elements in regions of interest and/or significant bathymetric variations and lower resolutions in regions of more homogeneous bathymetry, which reduced computational time.

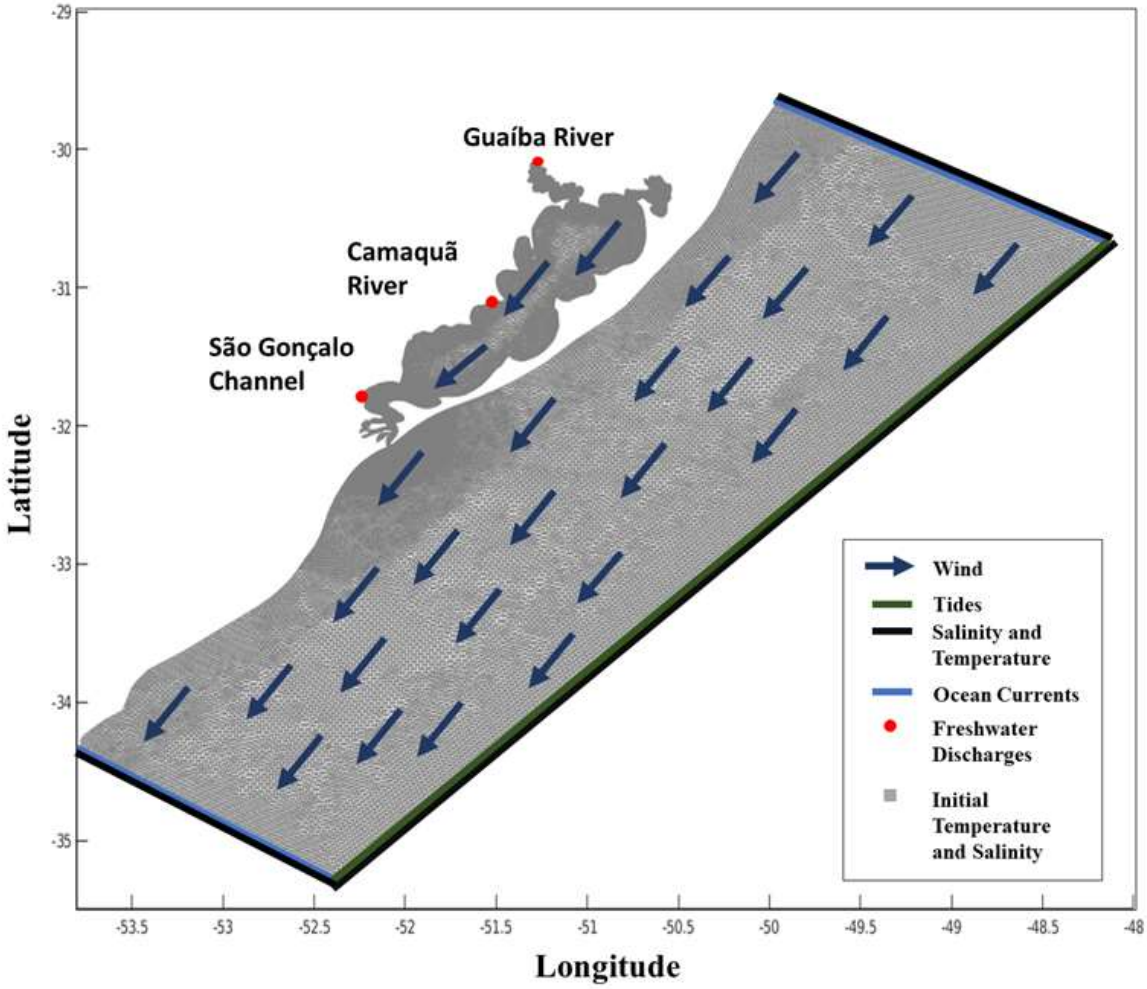

Figure 2: Numerical grid of the model domain with the location of open boundaries and an indication of the type of data used in each boundary.

Bathymetric data for Patos Lagoon and the adjacent coast were made available from the Directory of Hydrography and Navigation (DHN) and Rio Grande Port Authority, and were interpolated for the grid with the BlueKenue software. A triangular grid with 52098 nodes and 7 sigma layers resulted from the interpolation (Fig. 2). The model was initialized with salinity and temperature fields imposed on the domain considering the temperature of 24ºC for the whole domain, and salinity as 35 in the ocean and 0 inside the lagoon.

The model domain had three open continental boundaries, corresponding to the Guaíba and Camaquã rivers, and the São Gonçalo channel, aside from the ocean open boundary and the surface boundary. Temperature and salinity data for the ocean boundary were obtained from HYCOM + NCODA (Hybrid Model Coordinate Oceanic, https://www.hycom.org/), with a spatial resolution of 1/12º and temporal resolution of 3 h. The sea surface height and current velocity from tides input were retrieved from TPXO Project and imposed in the ocean boundary. The wind data (*u* and *v* components) were gathered from the European Center for Medium-Range Weather Forecasts (ECMWF, https://www.ecmwf.int) with a temporal resolution of 6 h and 0.75º of spatial resolution. The data were interpolated at the surface boundary for all the model domains.

The daily averaged freshwater discharge for the continental boundaries for each studied period were obtained from the Agência Nacional de Águas (ANA, https://www.ana.gov.br) for Guaíba and Camaquã rivers. Since there were no available freshwater discharge time series for the São Gonçalo channel, it was used the average of 700 m^3s^{-1} according to Vaz et al. (2006).

2.1 Hydrodynamic model calibration and validation

TELEMAC-3D was previously calibrated and validated for Patos Lagoon (Marques et al., 2010; Bitencourt et al., 2020b; Fernandes et al., 2021). The grid used in this work w as calibrated for the year 2011 using current velocity magnitude and direction data from the Praticagem station. Data was obtained with an ADCP (Acoustic Doppler Profiler) with a temporal resolution of 1 h. Model results and field data were compared by calculating the RMAE (Root Mean Absolute Error) and RMSE (Root Mean Square Error). RMAE values at the surface and at 13 m depth (0.06 and 0.14, respectively) show an excellent model reproduction (Walstra et al., 2001), so does the RMSE values,

both (0.31 for surface and 0.19 for 13 m depth) had values close to 0 (Fig. 3). The best model reproduction was obtained with the following set of $3.0*10^{-6}$ for wind coefficient, 30 for the horizontal diffusion coefficient, and $1.0*10^{-6}$ for vertical diffusion coefficient. The validation exercise was carried out based on the best set of physical parameters obtained in the calibration exercise, for the 2017 salinity data from both the Cassino Project and PELD Project (https://peld.furg.br). data set. According to the RMAE and RMSE (7.37 and 0.228, respectively), the model showed a good reproduction (Fig. 4).

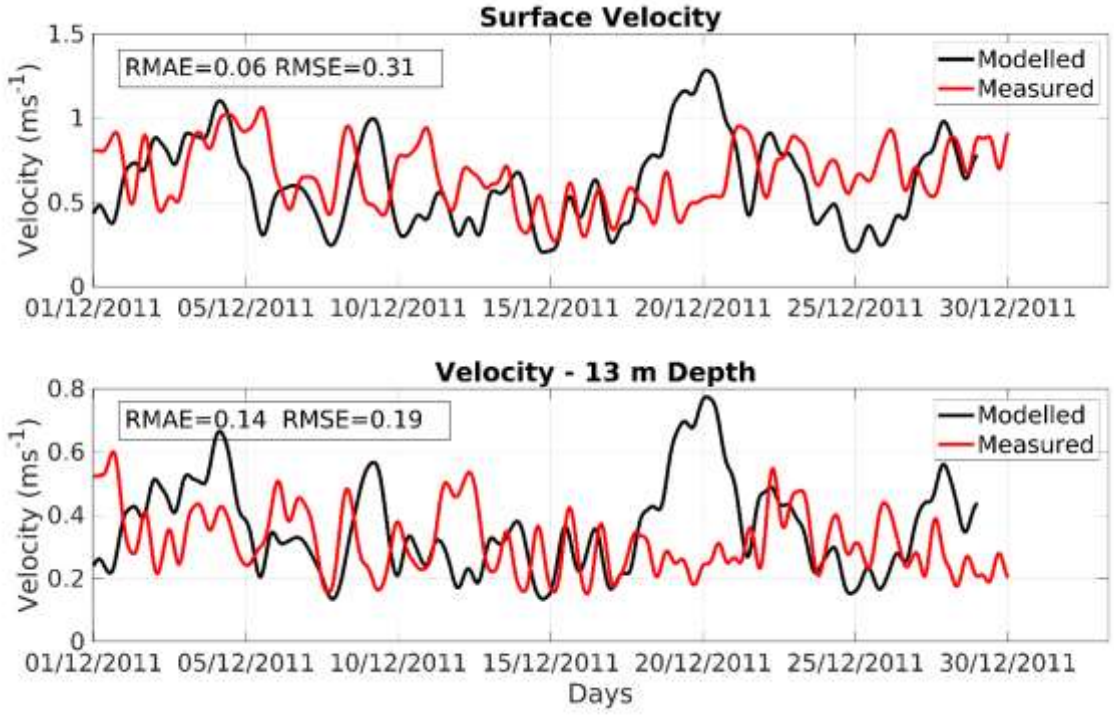

Figure 3: Model calibration exercise based on the comparison between measured current velocity (red) at Praticagem station and modeled current velocity(black) for December 2011. A) Current velocity at the surface B) Current velocity at 13m depth [modified from Fernandes et al. (2021)].

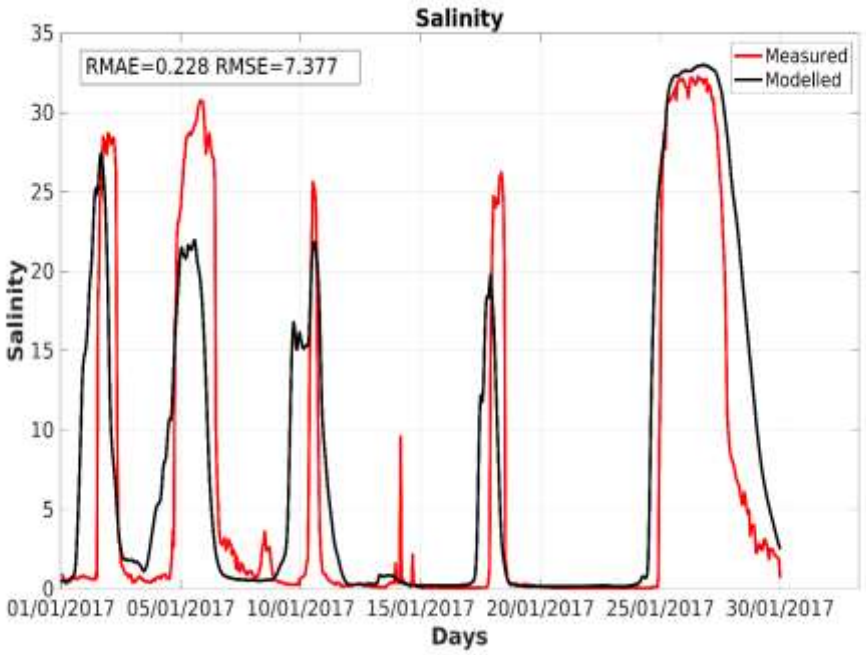

Figure 4: Model validation exercise based on the comparison between measured salinity (red) at PELD station and modeled salinity (black) from January 2017, both at 4 m depth [modified from Fernandes et al. (2021)].

2.1 Lagrangian module

Coupled with the hydrodynamic model, TELEMAC had a Lagrangian subroutine for the simulation of particle tracking. After selecting the number of drogues and their origin (Fig. 1), the hydrodynamic model computed the advection of each particle for each time step. The model allowed to discriminate active and passive drogues. The former drogue class had an active characteristic altering or being altered by the remaining variables of the model, such as temperature and salinity. Meanwhile, the passive drogue responded exclusively to the advection of the fluid. In this work, passive drogues were chosen because there were small variations of salinity and temperature across the major part of Patos Lagoon.

2.2 Model experiments

The Oceanic Niño Index (ONI) is an index used by the Climate Prediction Center (NOAA) to identify the cold and warm periods of ENSO. A variation of more than 0.5ºC from the average temperature in the Niño 3.4 region indicates an El Niño event

(+0.5ºC) or La Niña event (–0.5ºC). Based on this index, nine austral summer periods were selected for this study (from 2008 to 2017), which resulted in three austral summers for each ENSO condition (El Niño, Neutral, and La Niña). The austral summers of 2008/09, 2010/11 and 2011/12 were classified as La Niña, while of 2009/10, 2014/15, and 2015/16 were classified as El Niño and the austral summers of 2012/13, 2013/14, and 2016/17 as under Neutral Conditions.

All experiments were restricted to four months of simulation (from the beginning of December up to the ending of March, henceforth as Austral summer), considering an initial extra month of model spin-up (November). After running the hydrodynamic simulation for every simulated scenario, 7056 drogues were prescribed in the Lagrangian module divided into three stations in each lagoon cell (Fig. 1), where each drogue represented a colony of cyanobacteria. Since the goal of the study was to understand the transport of buoyant cyanobacteria during the austral summer and subject to ENSO cycle effects, all drogues were kept on the water surface, with no vertical transport.

2.3 Data Analysis

To better understand the dynamics of *Microcystis* spp. within the lagoon, we first investigated the drogue exportation for each time step, counting the drogues inside and outside the lagoon. The final rate of exportation was calculated using only the drogues that did not show any missing values that could lead to overestimation of exported drogues since missing values count as outside the lagoon.

The margin accumulation analyses were carried out for each cell. A polygon was built with 2 km inside the lagoon, divided into the west and east margins. For each time step, the drogues were counted inside each margin for each cell; also, all the drogues with missing values were dismissed. Both results were constrained with wind and river discharges for the same study period. The São Gonçalo channel flow was rather constant in all scenarios, with the same flow rate. Because of that, this latter data was not considered a variable, and it was excluded from the data analysis. Furthermore, the estuary portion was excluded from this analysis to track the bloom only across the freshwater portion of the Patos Lagoon.

3 Results

3.1 Patos lagoon hydrodynamics

In general, winds from the first quadrant were more frequent in all scenarios, except for the summer of 2010/11, when east-southeast winds took the majority of wind counts (more than 20%) compared to the remaining directions. (Fig. 5). Southern winds were evident in the austral summers of 2014/15, 2015/16, and 2016/2017. The mean wind velocity during all the simulated austral summers varied from 5.90 ms^{-1} in 2014/15 to 6.42 in 2008/09, although the austral summers of 2011/12 and 2015/16 were similar to those velocities (5.95 ms^{-1} and 6.40 ms^{-1}, respectively) (Table 1). The maximum wind velocity was observed in the austral summer of 2015/16 (15.92 ms^{-1}).

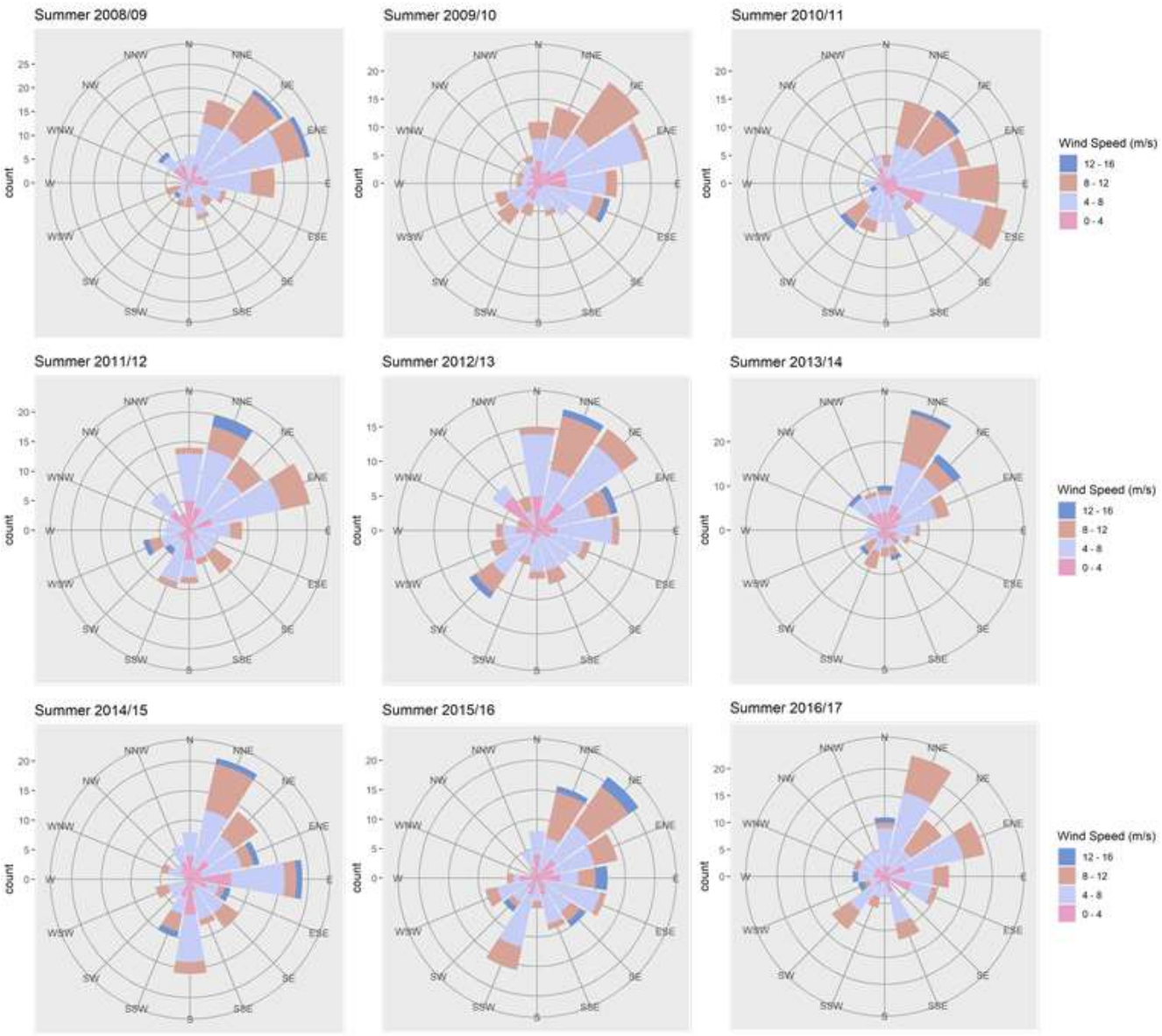

Figure 5: Wind frequency distribution for all the nine simulates austral summers based on wind velocity and direction data from the ECMWF.

The summer of 2011/12 was characterized by the lower mean discharge for both rivers (Table 2). The higher discharges were for Camaquã and Guaíba were observed in the summer of 2015/16, whereas a higher mean for both tributaries to the Patos Lagoon was determined for the summer of 2009/10. Furthermore, El Niño summers had the highest river discharge (2150.17 m^3s^{-1}) followed by 1318.87 m^3s^{-1} in the Neutral Condition, and by La Niña conditions with a flow of 595.30 m^3s^{-1}.

The wind and river discharge conditions are responsible for the mean hydrodynamic behavior presented in Figure 6, which presents mean current velocities for all the nine simulated austral summers. The lagoon western margin showed higher current velocity

in the central cell (C2), while the north cell (C1) had higher current velocities close to Guaíba River, except on the summers of 2011/12 (La Niña) and 2012/13 (Neutral Condition). On the eastern margin of the lagoon, higher velocities were also observed in the north cell (C1), especially during the three first austral summers analyzed. In all nine austral summers, the south cell of the lagoon (C3) had higher velocities on the eastern margin. The northwest part of the cell, however, also had higher current velocities notably in 2008/09 and 2010/11, both La Niña austral summers.

Table 1: Mean, maximum (Max) and minimum (Min) wind velocity for each austral summer

Wind (ms^{-1})			
Summer	**Mean**	**Max**	**Min**
2008/09	6.42	13.24	0.71
2009/10	6.12	12.62	0.33
2010/11	6.28	14.16	0.68
2011/12	5.95	13.66	0.62
2012/13	6.15	13.90	0.90
2013/14	6.08	13.53	1.00
2014/15	5.90	14.18	0.44
2015/16	6.40	15.92	0.23
2016/17	6.21	13.84	0.19

Table 2: Mean, maximum (Max), and minimum (Min) river discharge for each austral summer. Numbers in bold refer to the higher and the lower values.

River Discharge (m^3s^{-1})						
	Guaíba			Camaquã		
Summer	Mean	Max	Min	Mean	Max	Min
2008/09	626.9	1651.5	291.2	131.5	631.46	44.0
2009/10	**2424.0**	5843.6	445.4	**329.5**	1441.5	**69.0**
2010/11	770.9	5929.0	326.9	76.0	1022.8	25.0
2011/12	**387.1**	**1152.6**	**180.5**	**56.0**	**248.13**	**24.0**
2012/13	876.8	2237.7	267.6	92.0	585.37	29.0
2013/14	831.8	2157.4	278.8	294.6	1845.2	67.0

2014/15	1790.8	4423.0	394.4	228.4	554.5	38.0
2015/16	2235.7	**7782.4**	**564.1**	260.5	**2114.3**	56.0
2016/17	1334.0	3246.8	546.0	202.5	1959.4	39.0

Recirculation cells (eddies) were observed in all three cells of the main lagoon. The north cell (C1) showed a clockwise circulation at the center of the cell and a minor anticlockwise circulation located in the NE, while the central (C2) and south (C3) cells had a major anticlockwise circulation close to the center of the cell, and a minor clockwise circulation at the southeast. During 2009/10 austral summer (El Niño) the minor eddy from central (C2) and south (C3) lagoon, as well as the major eddy from the south (C3) were suppressed

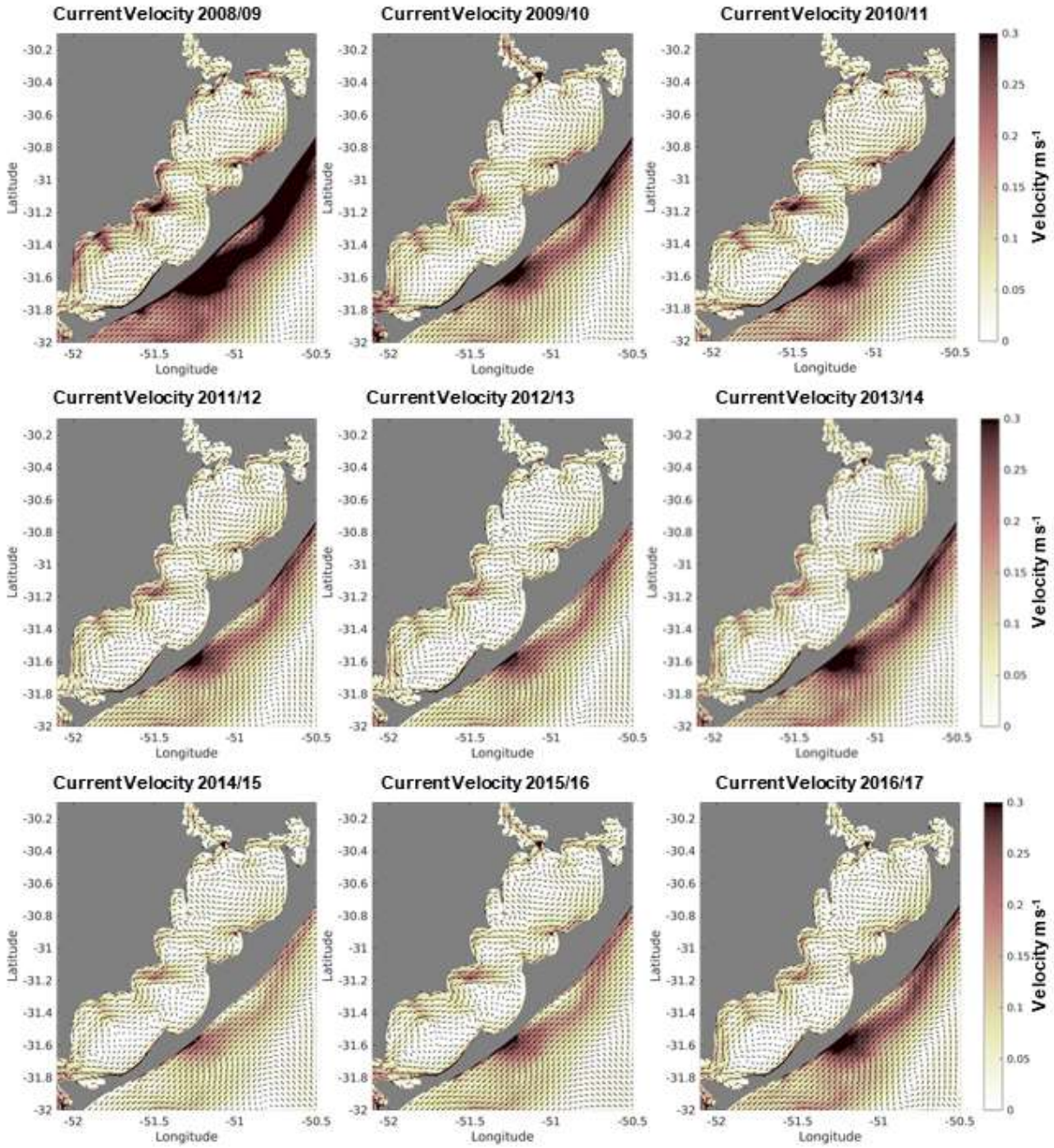

Figure 6: Mean current velocity for each austral summer. The color scale represents current intensity and vectors indicate current direction

3.1 Cyanobacteria export to the sea

From all nine simulated scenarios, only 2015/16 austral summer exported more than 50% of the prescribed cyanobacteria after the four months experiment (Table 3) followed by the austral summer of 2009/10. Export was higher under El Niño (Fig. 7) and Neutral Condition years (Fig. 8). On the other hand, La Niña years (Fig. 9) were

responsible for the lowest exportation among all nine scenarios, being 2008/09 with only 6% of the cyanobacteria exported to the sea (Table 3).

Table 3: Cyanobacteria export after four months of simulation for each austral summer period from 2008/09 to 2016/17, inside and outside the Patos Lagoon. Total cyanobacteria retained inside Patos Lagoon is represented by a percentage of traped drogues related to the total drogues at the end of each simulation.

Summer	**2008/09**	**2009/10**	**2010/11**	**2011/12**	**2012/13**	**2013/14**	**2014/15**	**2015/16**	**2016/17**
Inside the lagoon	5907.0	543.0	5327.0	5092.0	5187.0	5224.0	4560.0	460.0	3788.0
Export	377.0	484.0	459.0	414.0	543.0	615.0	754.0	895.0	1178.0
%	**94.0**	52.9	**92.1**	**92.5**	90.5	89.5	85.8	33.9	76.3

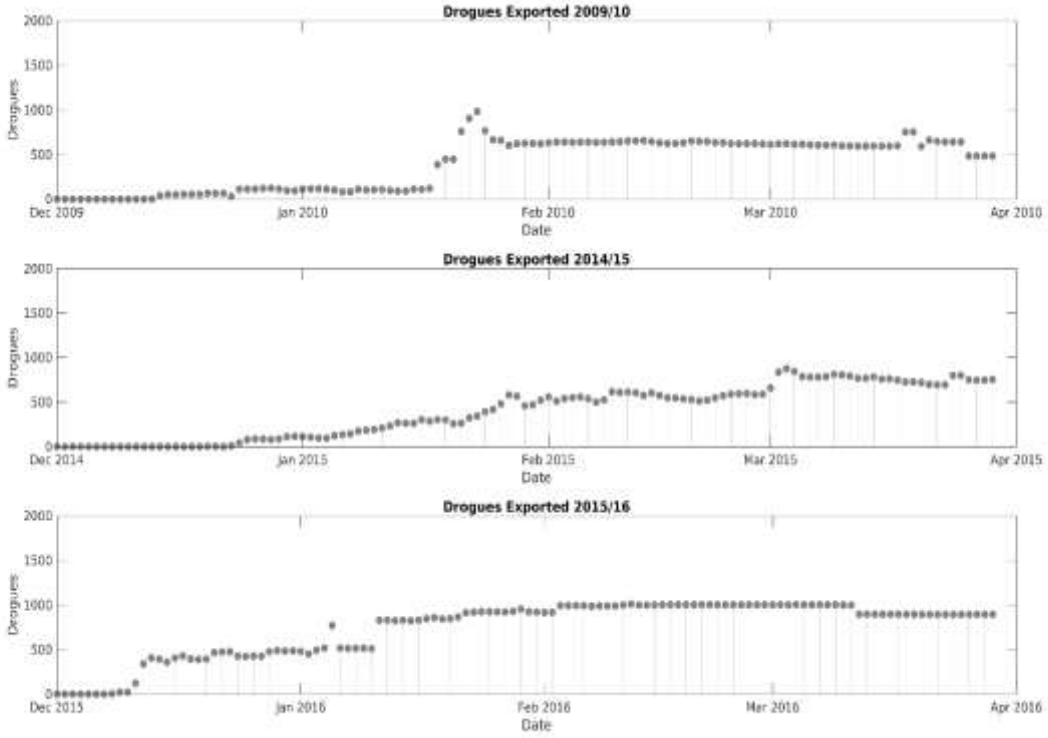

Figure 7: Cyanobacteria export during the austral summers corresponding to El Niño events

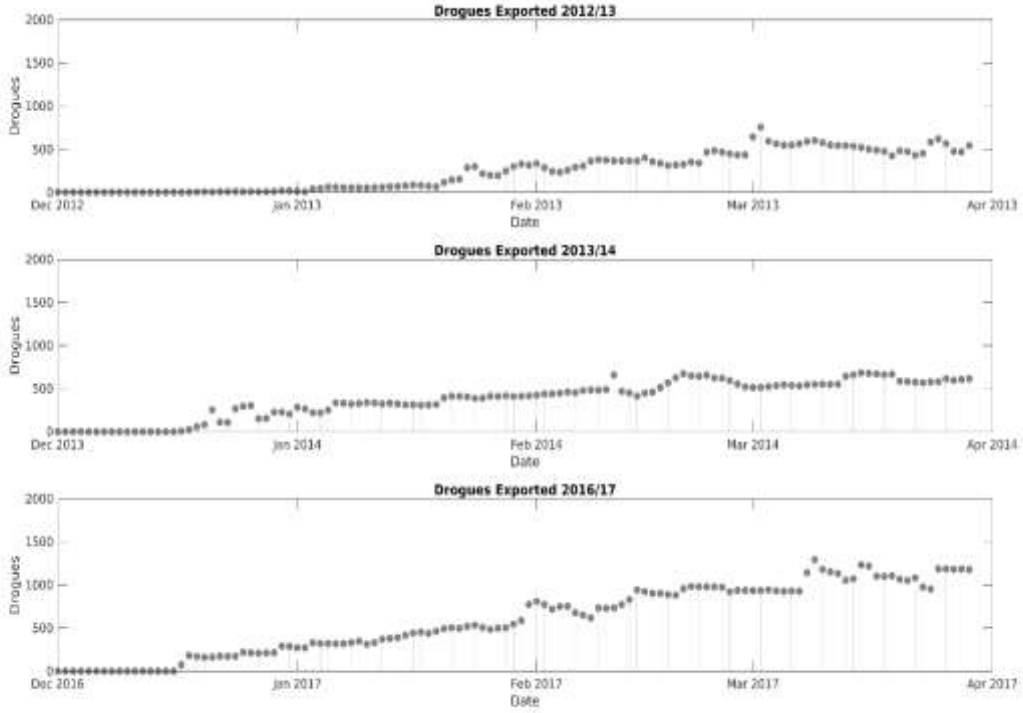

Figure 8: Cyanobacteria export during the austral summers corresponding to La Niña events

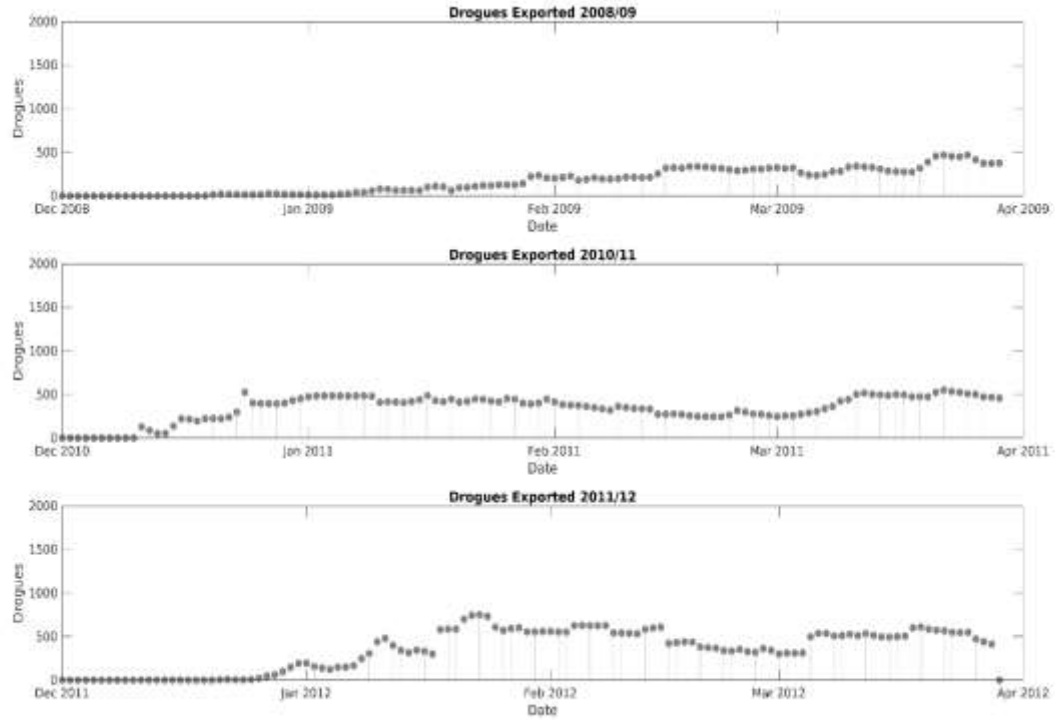

Figure 9: Cyanobacteria export during the austral summers corresponding to Neutral Condition events.

3.2 Cyanobacteria accumulation

All three cells in the main lagoon showed a particular pattern, even when compared with the different meteoceanographic conditions imposed by ENSO cycles. The northern cell (C1) accumulated cyanobacteria on the western margin for all the nine simulated scenarios, with higher accumulation during 2008/09 summer (Fig. 10), followed by 2011/12 and 2014/15 (not shown). The summer of 2015/16 (Fig. 11) had the lower accumulation on the eastern margin while the summer of 2016/17 (Fig. 12) for the western margin. Furthermore, the higher accumulation on the eastern margin was observed in 2011/12 and 2008/09, both La Niña summers.

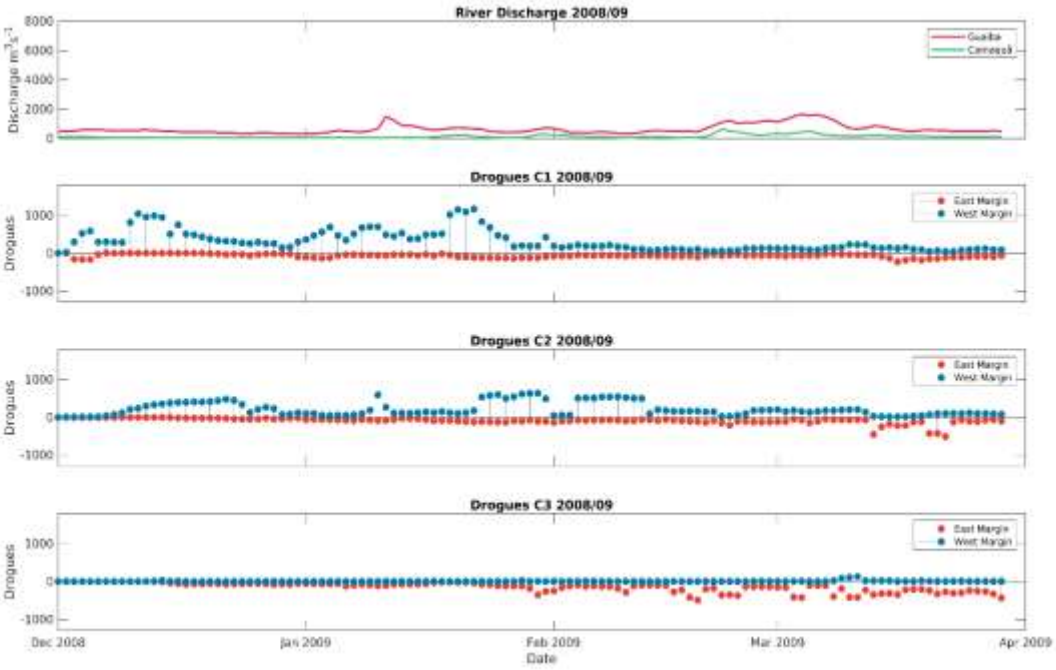

Figure 10: A) River discharge during the austral summer of 2008/09. Guaíba river in red and Camaquã river in green. Cyanobacteria on the east margin are in red and on the west margin in blue, B) North cell, C) Central cell and D) south cell of Patos Lagoon

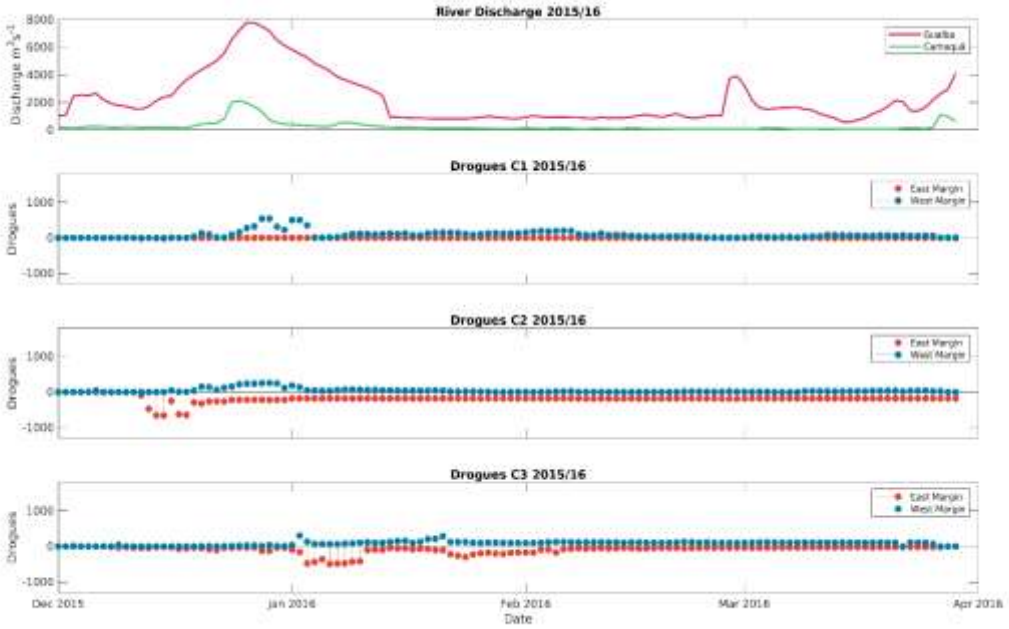

Figure 11: A) River discharge during the austral summer of 2015/16. Guaíba river in red and Camaquã river in green. Cyanobacteria on the east margin are in red and on the west margin in blue, B) North cell, C) Central cell and D) south cell of Patos Lagoon

The accumulation of cyanobacteria on the central cell (C2) did not show the same behavior as in the north cell (C1) (Fig. 10-12). The austral summer of 2015/16 had the higher accumulation on the west margin and the lower on the east margin.

The summer of 2016/17 (Fig. 12) presented the higher cyanobacteria accumulation on the eastern margin and low accumulation on the western margin in the south cell (C3). Compared to the other two cells, the southern cell had the higher difference between the margins, the eastern having 10 times more chance of cyanobacteria accumulation than the western margin. The accumulation on the western margin prevails in the summers of 2015/16 (Fig. 11) and 2009/10 (not shown), with the summer of 2015/16 having the lower concentration of cyanobacteria in the eastern margin, in opposition to the remaining summers.

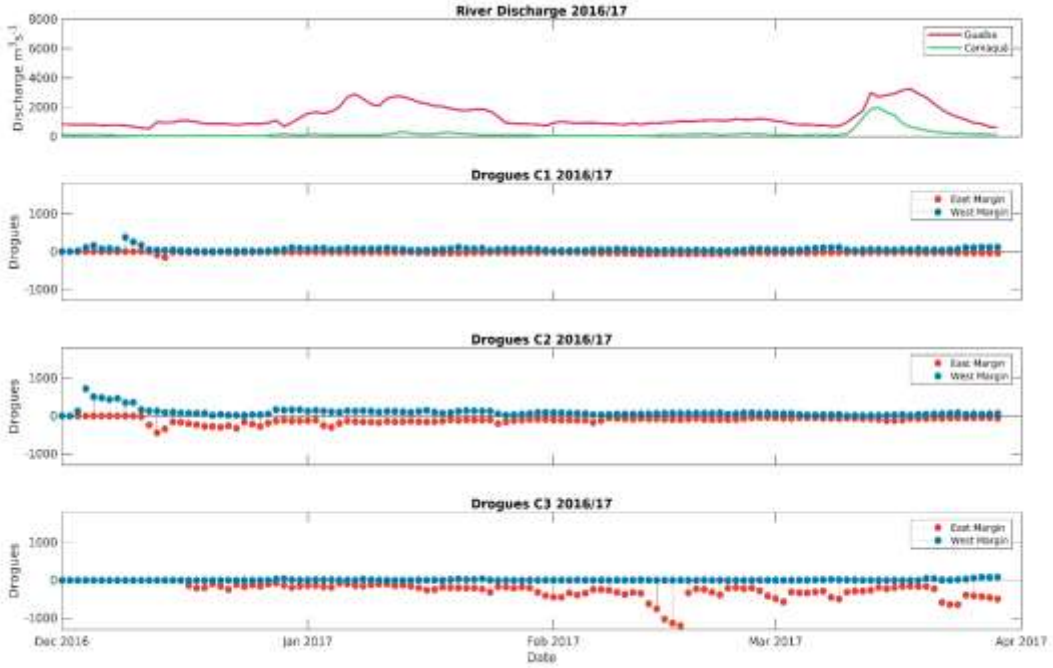

Figure 12: A) River discharge during the austral summer of 2016/17. Guaíba river in red and Camaquã river in green. Cyanobacteria on the east margin are in red and on the west margin in blue, B) North cell, C) Central cell and D) south cell of Patos Lagoon

4 Discussion

The presented models results represent cyanobacteria colonies during austral summers from 2008 to 2017. Results were subject to the lagoon hydrodynamics under different ENSO scenarios. Simulations are consistent with previous works carried out in Patos Lagoon (Möller et al., 2001; Fernandes, 2002), with the predominance of northwest winds and occasionally southern winds, especially in the austral summer of 2010/11, identified as a La Niña summer.

The results of the simulations showed the already heavily discussed pattern of ENSO effects on hydrodynamics in the region, which consists of high river discharge and lagoon flow towards the ocean during El Niño events, and higher residence time during La Niña events (Fernandes et al., 2002; Marques, 2012; Bitencourt et al., 2020a; Távora et al., 2020). River discharges play an important role in the lagoon circulation and become even more important during El Niño summers, due to the precipitation anomaly

associated with ENSO (Barros and Marques, 2012; Fernandes et al., 2002). During La Niña summers, especially of 2009/10 and 2015/16, the river discharge is low.

The mean summer hydrodynamics showed concentric recirculation cells inside all three cells of the lagoon, analogous to what was observed by Moller et. al. (1996) and Bortolin et al. (2020). during NE winds. Contrarily, the action of SW winds tends to alter the circulation pattern (Moller et al., 1996, Bortolin et al., 2020), however, in none of the nine simulated summers it persisted long enough to change the pattern observed in the summer mean circulation. The summer of 2009/10, however, despite showing a similar pattern, suppressed the minor gyres from the cells as a result of the high mean river discharge (see Table 2). The same result was not observed for the summer of 2015/16, even though the average river flow was above 2000 m^3s^{-1}, overcoming the wind influence as proposed by Möller and Castaing (1999). It is worth noticing that despite the high mean value, the flow of 2015/16 was irregularly distributed during the summer (see Fig.11), possibiliting the wind dominance from late January throw February. Also, this summer had more southern winds occurrences, with higher velocities (see Fig. 5) than the summer of 2009/10, which is known to suppress seaward flow (Möller et al., 2001; Bitencourt et al., 2020a; Távora et al., 2020). Nonetheless, both summers had the higher cyanobacteria export to the coast. The positive precipitation anomaly related to El Niño promotes the advection of phytoplankton for the coastal region (Odebrecht et al., 2015), as observed for the transportation of harmful *Microcystis* spp. blooms to the Uruguayan coastal beaches (Pírez et al., 2013). During La Niña austral summers the opposite happened (de Souza et al., 2018) and the cyanobacteria were trapped inside the lagoon. Therefore the bloom remained inside the lagoon for a longer period, which can benefit the production of the toxin (Matthiensen et al., 1999). According to Devercelli (2010), La Niña events are responsible for higher algal density and biovolume phytoplankton dilution due to rainfall reflects on toxin dilution (Reichwaldt and Ghadouani, 2012), which must be taken into account when monitoring susceptible HABs areas. On the other hand, the influence of rainfall in cyanobacteria is more complicated when added the biological variables are into the calculation. Low rainfall periods have a positive effect on cyanobacteria, especially *Microcystis* spp., with bloom persevering under dry conditions, and low wind velocities (Reichwaldt and Ghadouani, 2012). Also, the high tolerance ability of *Microcystis* spp. allows its colonies to remain growing on low to

medium (salinity varying from 9 to17) salinity rates (Reichwaldt and Ghadouani, 2012), which means that not only *Microcystis* app. blooms can be transported to the estuary region of Patos Lagoon, but it possibly continues to grow for a short period. The same authors discussed the effect of irregularly distributed rainfall, which can cause higher pulses of nutrients into the water is favorable to cyanobacterial growth, an aspect that can be enhanced by climate change (Paerl, 2017).

However, rainfall and river discharge are not the only physical forcing controlling the Patos Lagoon dynamics, as NE winds favor flood flows towards the coast and southern winds can promote salt inflow (Bitencourt et al., 2020a; Távora et al., 2020). Thus, when focusing on the estuary, the presence of southern winds, a long retention time of cyanobacteria in the summers of 2010/11, 2014/15, and 2016/17 (see Fig. 5) could be partially responsible for holding the cyanobacteria inside the lagoon. This might have been the case for 2014/15 summer (El Niño) (Fig. 7). Also, this summer period had lower river discharge in comparison to the other two El Niño summers. There was no significant difference in the cyanobacteria export among those three El Niño summer periods, however, as shown by Belarmino et al. (2021) and Reis-Santos et al. (2021) moderate and weak El Niño events (2009/10 and 2014/15, respectively; classification by Golden Gate Weather Services, 2021) affect Patos Lagoon differently than very strong El Niño events (as 2015/16). The percentage of cyanobacteria trapped inside Patos Lagoon during El Niño events reflects the intensity, the higher the intensity, the higher the cyanobacteria export.

The accumulation process caused by wind-driven currents was also already observed in Río de La Plata during mean flow rates (Aubriot et al., 2020). At the same time, other works highlighted that wind action promotes patches formation (Deng et al., 2016; Wang et al., 2016).

The predominance of northern winds on every simulated scenario promoted the cyanobacteria accumulation on the western margin of the northern and central cells (C1 and C2, respectively). The austral summer of 2008/2009 had strong and frequent winds from the north quadrant (Fig. 5) that reflected on the cyanobacteria accumulation on the western margin of the lagoon (in C1 and C2, Fig. 10). Meanwhile, the south cell of the lagoon (C3) had little to no accumulation on the western margin in any of the simulated scenarios, showing that the southern cell accumulation on the western margin is not connected with the wind or river discharge, while the eastern margin of the south cell

(C3) accumulates cyanobacteria on every austral summer, especially 2011/2012 (La Niña) and 2013/2014 (Neutral Condition).

The high export rate from El Niño years might explain the lack of accumulation in the south cell (C3) during the El Niño austral summer, considering that C3 has the lower residence time of all three cells (Aguilera et al., 2020), and probably this residence time reduces on high river discharges events (Fernandes et al., 2002).

Thus, results from the modeling experiments suggest that the Northern winds will accumulate *Microcystis spp.* colonies on the western margin, especially in the north (C1) and central (C2) Patos Lagoon cells. However due to a few exceptions, especially under southern winds and La Niña influenced austral summers, both margins of the south cell (C3) may accumulate *Microcystis spp.* Colonies

5 Conclusion

This study tested a Lagrangian approach to identify the susceptible accumulation sites for *Microcystis* inside Patos Lagoon focusing on the influence of ENSO cycles. Results here presented showed that cyanobacteria export occurs every austral summer, with higher export values during El Niño events. Otherwise, La Niña events can hold up to 94% of cyanobacteria inside the lagoon, even having the same average circulation as El Niño events.

The cyanobacteria accumulation on both margins is higher in La Niña and Normal Condition austral summers, due to the low river discharges, and its transport across the lagoon is more related to winds rather than to the river discharge. While the wind accumulates and transports the colonies inside the lagoon, the river discharge exports them.

The most susceptible places for the accumulation of cyanobacteria are the western margin of the northern and central cells (C1 and C2, respectively) and the eastern margin of the south cell (C3). The northern winds are responsible for the accumulation of the two northern cells, while southern winds trap the cyanobacteria colonies inside the estuary in average/low river discharge events.

These results are the first step forward towards the monitoring of these regions with a higher risk of harmful blooms. However, further studies considering a biological model with vertical cyanobacterial transport are necessary due to the *Microcystis* seasonal life cycle.

Acknowledgments

The authors thank the Federal University of Rio Grande – FURG and the Brazilian Improving Coordination of Higher Education Personnel – CAPES for their support and financial aid. We thank CAPES for the research grant 88887.342873/2019-00 (BFC)

References

Aguilera, L., Santos, A.L.F. Dos, Rosman, C.P.C., 2020. On characteristic hydraulic times through hydrodynamic modelling : discussion and application in Patos Lagoon (RS). Rev. Ambient. Água 15. https://doi.org/10.4136/1980-993X

Aleynik, D., Dale, A.C., Porter, M., Davidson, K., 2016. A high resolution hydrodynamic model system suitable for novel harmful algal bloom modelling in areas of complex coastline and topography. Harmful Algae 53, 102–117. https://doi.org/10.1016/j.hal.2015.11.012

Aubriot, L., Zabaleta, B., Bordet, F., Sienra, D., Risso, J., Achkar, M., Somma, A., 2020. Assessing the origin of a massive cyanobacterial bloom in the Río de la Plata (2019): Towards an early warning system. Water Res. 181, 115944. https://doi.org/10.1016/j.watres.2020.115944

Barros, G.P., Marques, W.C., 2012. Long-term temporal variability of the freshwater discharge and water levels at Patos Lagoon, Rio Grande do Sul, Brazil. Int. J. Geophys. 2012. https://doi.org/10.1155/2012/459497

Belarmino, E., Francisco de Nóbrega, M., Grimm, A.M., da Silva Copertino, M., Vieira, J.P., Garcia, A.M., 2021. Long-term trends in the abundance of an estuarine fish and relationships with El Niño climatic impacts and seagrass meadows reduction. Estuar. Coast. Shelf Sci. 261. https://doi.org/10.1016/j.ecss.2021.107565

Bitencourt, L.P., Fernandes, E., Möller, O., Ross, L., 2020a. The contribution of ENSO cycles to the salinity spatio-temporal variability in a bar-built microtidal estuary.

Reg. Stud. Mar. Sci. 40, 101496. https://doi.org/10.1016/j.rsma.2020.101496

Bitencourt, L.P., Fernandes, E.H., da Silva, P.D., Möller, O., 2020b. Spatio-temporal variability of suspended sediment concentrations in a shallow and turbid lagoon. J. Mar. Syst. 212. https://doi.org/10.1016/j.jmarsys.2020.103454

Bortolin, E.C., Weschenfelder, J., Fernandes, E.H., Bitencourt, L.P., Möller, O.O., García-Rodríguez, F., Toldo, E., 2020. Reviewing sedimentological and hydrodynamic data of large shallow coastal lagoons for defining mud depocenters as environmental monitoring sites. Sediment. Geol. 410, 105782. https://doi.org/10.1016/j.sedgeo.2020.105782

de Souza, M.S., Muelbert, J.H., Costa, L.D.F., Klering, E. V., Yunes, J.S., 2018. Environmental Variability and Cyanobacterial Blooms in a Subtropical Coastal Lagoon: Searching for a Sign of Climate Change Effects. Front. Microbiol. 9, 1–12. https://doi.org/10.3389/fmicb.2018.01727

Deng, J., Chen, F., Liu, X., Peng, J., Hu, W., 2016. Horizontal migration of algal patches associated with cyanobacterial blooms in an eutrophic shallow lake. Ecol. Eng. 87, 185–193. https://doi.org/10.1016/j.ecoleng.2015.12.017

Devercelli, M., 2010. Changes in phytoplankton morpho-functional groups induced by extreme hydroclimatic events in the Middle Paraná river (Argentina). Hydrobiologia 639, 5–19. https://doi.org/10.1007/s10750-009-0020-6

Fernandes, E.H.L., Dyer, K.R., Moller, O.O., Niencheski, L.F.H., 2002. The Patos Lagoon hydrodynamics during an El Niño event (1998). Cont. Shelf Res. 22, 1699–1713. https://doi.org/10.1016/S0278-4343(02)00033-X

Fernandes, E.H.L., Mariño-Tapia, I., Dyer, K.R., Möller, O.O., 2004. The attenuation of tidal and subtidal oscillations in the Patos Lagoon estuary. Ocean Dyn. 54, 348–359. https://doi.org/10.1007/s10236-004-0090-y

Fernandes, E.H.L., da Silva, P.D., Gonçalves, G.A., Moller, O.O., 2021. Dispersion Plumes in Open Ocean Disposal Sites of Dredged Sediment. Water 1–20. https://doi.org/10.3390/w13060808

Golden Gate Weather Services, 2020. El Niñno and La Niña years and intensities. Based on oceanic Ni˜no index (ONI). Updated Aug-Set, 2021 Available in. http://ggweather. com/enso/oni.htm.

Grimm, A.M., Ferraz, S.E.T., Gomes, J., 1998. Precipitation anomalies in southern Brazil associated with El Nino and La Nina events. J. Clim. 11, 2863–2880. https://doi.org/10.1175/1520-0442(1998)011<2863:PAISBA>2.0.CO;2

Hallegraeff, G., Enevoldsen, H., Zingone, A., 2021. Global harmful algal bloom status reporting. Harmful Algae 102. https://doi.org/10.1016/j.hal.2021.101992

Havens, H., Luther, M.E., Meyers, S.D., Heil, C.A., 2010. Lagrangian particle tracking of a toxic dinoflagellate bloom within the Tampa Bay estuary. Mar. Pollut. Bull. 60, 2233–2241. https://doi.org/10.1016/j.marpolbul.2010.08.013

Hervouet, J.M., 2007. Hydrodynamics of Free Surface Flows: Modelling with the finite element method, John Wiley & Sons Ltd. https://doi.org/10.1002/9780470319628

Kjerfve, B., 1986. Comparative Oceanography of Coastal Lagoons. Estuar. Var. 63–81. https://doi.org/10.1016/b978-0-12-761890-6.50009-5

Kruk, C., Martínez, A., Martínez de la Escalera, G., Trinchin, R., Manta, G., Segura, A.M., Piccini, C., Brena, B., Yannicelli, B., Fabiano, G., Calliari, D., 2021. Rapid freshwater discharge on the coastal ocean as a mean of long distance spreading of an unprecedented toxic cyanobacteria bloom. Sci. Total Environ. 754, 142362. https://doi.org/10.1016/j.scitotenv.2020.142362

Liu, H., Zheng, Z.C., Young, B., Harris, T.D., 2019. Three-dimensional numerical modeling of the cyanobacterium Microcystis transport and its population dynamics in a large freshwater reservoir. Ecol. Modell. 398, 20–34. https://doi.org/10.1016/j.ecolmodel.2019.01.022

Marques, W.C., 2012. The Temporal Variability of the Freshwater Discharge and Water Levels at the Patos Lagoon, Brazil. Int. J. Geosci. 03, 758–766. https://doi.org/10.4236/ijg.2012.34076

Marques, W.C., Fernandes, E.H., Monteiro, I.O., Möller, O.O., 2009. Numerical modeling of the Patos Lagoon coastal plume , Brazil 29, 556–571. https://doi.org/10.1016/j.csr.2008.09.022

Marques, W.C., Fernandes, E.H.L., Moraes, B.C., Möller, O.O., Malcherek, A., 2010. Dynamics of the Patos Lagoon coastal plume and its contribution to the deposition pattern of the southern Brazilian inner shelf 115, 1–22. https://doi.org/10.1029/2010JC006190

Matthiensen, A., Yunes, J.S., Codd, G.A., 1999. Ocorrência, distribuição e toxicidade de cianobactérias no estuário da Lagoa dos Patos, RS. Rev. Bras. Biol. 59, 361–376. https://doi.org/10.1590/s0034-71081999000300002

Matthiensen, A., Beattie, K.A., Yunes, J.S., Kaya, K., Codd, G.A., 2000. [D-Leu1]Microcystin-LR, from the cyanobacterium Microcystis RST 9501 and from a Microcystis bloom in the Patos Lagoon estuary, Brazil. Phytochemistry 55, 383–

387. https://doi.org/10.1016/S0031-9422(00)00335-6

Möller, O.O., Castaing, P., 1999. Hydrographical Characteristics of the Estuarine Area of Patos Lagoon (30°S, Brazil). Estuaries South Am. 83–100. https://doi.org/10.1007/978-3-642-60131-6_5

Moller, O.O., Lorenzzentti, J.A., Stech, J.L., Mata, M.M., 1996. The Patos Lagoon summertime circulation and dynamics. Cont. Shelf Res. 16, 335–351. https://doi.org/10.1016/0278-4343(95)00014-R

Möller, O.O., Castaing, P., Salomon, J.C., Lazure, P., 2001. The influence of local and non-local forcing effects on the subtidal circulation of Patos Lagoon. Estuaries 24, 297–311. https://doi.org/10.2307/1352953

O'Neil, J.M., Davis, T.W., Burford, M.A., Gobler, C.J., 2012. The rise of harmful cyanobacteria blooms: The potential roles of eutrophication and climate change. Harmful Algae 14, 313–334. https://doi.org/10.1016/j.hal.2011.10.027

Odebrecht, C., Seeliger, U., Coutinho, R., Torgan, L.C., 1987. Florações de Microcystis (cianobactérias) na Lagoa dos Patos. Simpósio sobre ecossistemas da costa sul e sudeste Bras. síntese dos conhecimentos.ACIESP, Cananéia 2, 280–287.

Odebrecht, C., Abreu, P.C., Carstensen, J., 2015. Retention time generates short-term phytoplankton blooms in a shallow microtidal subtropical estuary. Estuar. Coast. Shelf Sci. 162, 35–44. https://doi.org/10.1016/j.ecss.2015.03.004

Paerl, H.W., 2017. Controlling harmful cyanobacterial blooms in a climatically more extreme world: Management options and research needs. J. Plankton Res. 39, 763–771. https://doi.org/10.1093/plankt/fbx042

Paerl, H.W., Hall, N.S., Calandrino, E.S., 2011. Controlling harmful cyanobacterial blooms in a world experiencing anthropogenic and climatic-induced change. Sci. Total Environ. 409, 1739–1745. https://doi.org/10.1016/j.scitotenv.2011.02.001

Pírez, M., Gonzalez-sapienza, G., Sienra, D., Ferrari, G., Last, M., 2013. Limited analytical capacity for cyanotoxins in developing countries may hide serious environmental health problems : Simple and affordable methods may be the answer. J. Environ. Manage. 114, 63–71. https://doi.org/10.1016/j.jenvman.2012.10.052

Possamai, B., Vieira, J.P., Grimm, A.M., Garcia, A.M., 2018. Temporal variability (1997-2015) of trophic fish guilds and its relationships with El Niño events in a subtropical estuary. Estuar. Coast. Shelf Sci. 202, 145–154. https://doi.org/10.1016/j.ecss.2017.12.019

Qin, R., Lin, L., 2019. Integration of GIS and a Lagrangian particle-tracking model for Harmful Algal Bloom trajectories prediction. Water (Switzerland) 11. https://doi.org/10.3390/w11010164

Reichwaldt, E.S., Ghadouani, A., 2012. Effects of rainfall patterns on toxic cyanobacterial blooms in a changing climate: Between simplistic scenarios and complex dynamics. Water Res. 46, 1372–1393. https://doi.org/10.1016/j.watres.2011.11.052

Reis-Santos, P., Condini, M. V., Albuquerque, C.Q., Saint'Pierre, T.D., Garcia, A.M., Gillanders, B.M., Tanner, S.E., 2021. El Niño – Southern Oscillation drives variations in growth and otolith chemistry in a top predatory fish. Ecol. Indic. 121, 106989. https://doi.org/10.1016/j.ecolind.2020.106989

Reynolds, C.S., Jaworski, G.H.M., A., C.H., F., L.G., 1981. Philosophical Transactions of the Royal Society of London. Philos. Trans. R. Soc. London 95, 65–87.

Silva, L.M., 2005. Ocorrência de Cianobactérias no Estuário e Costa Adjacente à Lagoa dos Patos, Rio Grande, RS: avaliação preliminar dos riscos À balneabilidade. FURG.

Solari, L.C., Gabellone, N.A., Claps, M.C., Casco, M.A., Quaíni, K.P., Neschuk, N.C., 2014. Phytoplankton chlorophyte structure as related to ENSO events in a saline lowland river (Salado River, Buenos Aires, Argentina). Ecol. Evol. 4, 918–932. https://doi.org/10.1002/ece3.983

Soontiens, N., Binding, C., Fortin, V., Mackay, M., Rao, Y.R., 2019. Algal bloom transport in Lake Erie using remote sensing and hydrodynamic modelling: Sensitivity to buoyancy velocity and initial vertical distribution. J. Great Lakes Res. 45, 556–572. https://doi.org/10.1016/j.jglr.2018.10.003

Távora, J., Fernandes, E.H., Bitencourt, L.P., Orozco, P.M.S., 2020. El-Niño Southern Oscillation (ENSO) effects on the variability of Patos Lagoon Suspended Particulate Matter. Reg. Stud. Mar. Sci. 40, 101495. https://doi.org/10.1016/j.rsma.2020.101495

They, N.H., Ferreira, L.M.H., Marins, L.F., Abreu, P.C., 2015. Bacterial Community Composition and Physiological Shifts Associated with the El Niño Southern Oscillation (ENSO) in the Patos Lagoon Estuary. Microb. Ecol. 69, 525–534. https://doi.org/10.1007/s00248-014-0511-5

Vaz, A.C., Möller jr, O.O., de Almeida., T.L., 2006. Análise quantitativa da descarga dos rios afluentes da Lagoa dos Patos. Atlântica 28, 13–23.

Vieira, J.P., Garcia, A.M., Grimm, A.M., 2008. Evidences of El Niño effects on the mullet fishery of the Patos Lagoon estuary. Brazilian Arch. Biol. Technol. 51, 433–440. https://doi.org/10.1590/s1516-89132008000200025

Walstra, D. J. R., Van Rijn, L. C., Blogg, H., & Van Ormondt, M. (2001, June). Evaluation of a hydrodynamic area model based on the COAST3D data at Teignmouth 1999. In *Proceedings of coastal dynamics 2001 conference, Lund D* (Vol. 4, pp. 1-D4).

Wang, H., Zhang, Z., Liang, D., du, H., Pang, Y., Hu, K., Wang, J., 2016. Separation of wind's influence on harmful cyanobacterial blooms. Water Res. 98, 280–292. https://doi.org/10.1016/j.watres.2016.04.037

Wu, X., Kong, F., Chen, Y., Qian, X., Zhang, L., Yu, Y., Zhang, M., Xing, P., 2010. Horizontal distribution and transport processes of bloom-forming Microcystis in a large shallow lake (Taihu, China). Limnologica 40, 8–15. https://doi.org/10.1016/j.limno.2009.02.001

Wynne, T.T., Stumpf, R.P., Tomlinson, M.C., Schwab, D.J., Watabayashi, G.Y., Christensen, J.D., 2011. Estimating cyanobacterial bloom transport by coupling remotely sensed imagery and a hydrodynamic model. Ecol. Appl. 21, 2709–2721. https://doi.org/10.1890/10-1454.1

Yunes, J.S., 2009. Florações de microcystis na lagoa dos patos e o seu estuário: 20 Anos de Estudos. Oecologia Bras. 13, 313–318. https://doi.org/10.4257/oeco.2009.1302.06

Yunes, J.S., Salomon, P., Matthiensen, A., Beattie, K.A., Raggett, S.L., Codd, G.A., 1996. Toxic blooms of cyanobacteria in the Patos Lagoon Estuary, southern Brazil. J. Aquat. Ecosyst. Heal. 223–229.

Capítulo VII: Considerações finais

Florações nocivas de cianobactérias estão presentes naturalmente na Lagoa dos Patos. Porém, a eutrofização e as mudanças climáticas tendem a modificar a dinâmica das cianobactérias, aumentando o risco de contaminação pelas florações.

O verão de 2019/20 foi caracterizado como um verão seco em comparação com dados históricos, permitindo o desenvolvimento de florações nocivas na parte límnica da Lagoa dos Patos, como mostram os resultados de NDCI nos quatro pontos estudados. As manchas presentes nas margens da lagoa tanto em Tavares (30 de dezembro) quanto em Arambaré (13 de janeiro) foram observadas nos altos valores de NDCI para o período, apesar de não estarem relacionadas com os picos de NDCI.

A dinâmica de vento e descargas fluviais aparenta ter modulado as florações do verão de 2019/20, já que a baixa vazão permitiu o desenvolvimento da floração, enquanto o vento transportou as manchas dentro da lagoa.

O modelo apresentado no segundo estudo corrobora o resultado do primeiro manuscrito, já que nos verões com maior descarga fluvial também ocorreram as maiores taxas de exportação de cianobactérias. Os ventos observados nos

verões de 2008 a 2017 foram responsáveis pelo transporte de cianobactérias dentro da lagoa e acumulação das mesmas nas margens.

De acordo com os resultados, as cidades a oeste da lagoa, principalmente na célula central (C2) são mais suscetíveis a acumulação de cianobactérias, devido a predominância de ventos NE em todos os cenários. É nesta célula que estão localizadas as cidades de Arambaré e Mostardas.

As células norte e sul (C1 e C3, respectivamente) apresentaram uma diferença maior na acumulação das margens, porém menos colônias acumularam nas margens destas células em comparação com a célula central (C2). A célula sul (C3) possui o menor tempo de residência entre as três (Aguilera *et al.*, 2020), enquanto a célula norte (C1), no modelo, possui apenas uma fonte de cianobactérias, não recebendo colônias de outras células. Desta maneira, a célula central (C2) que apresenta um tempo de residência maior que a C3 ao mesmo tempo que recebe as colônias da C1, além das colônias que iniciam na C2 durante o inicio da simulação, acaba tendo a maior acumulação de cianobactérias na margem.

Os eventos relacionados ao ENSO influenciaram a exportação de cianobactérias para área adjacente, apesar de não ter apresentado diferenças significativas. Verões de El Niño tendem a exportar mais cianobactérias para o oceano, e consequentemente diminuir a acumulação na célula norte (C1). As células central e sul acabam acumulando cianobactérias que foram exportadas pela C1.

Cidades como São José do Norte, localizada na célula sul (C3) ao lado leste da lagoa, está suscetível a acumulação de cianobactérias inclusive nos anos El

Niño, já que as colônias das células superiores acabam descendo em direção ao oceano.

Apesar dos métodos utilizados neste trabalho não identificarem diretamente a espécie encontrada nas florações, assim como a falta de informação sobre nutrientes na parte límnica da lagoa, os resultados apresentados demonstram como a dinâmica das florações de cianobactérias potencialmente nocivas é influenciada por vento e descarga fluvial, facilitando a definição dos pontos de maior risco para a acumulação da floração.

Referências Bibliográficas

Aguilera, L, Santos, ALF Dos, Rosman, CPC (2020) On characteristic hydraulic times through hydrodynamic modelling : discussion and application in Patos Lagoon (RS). Rev. Ambient. Água 15. https://doi.org/10.4136/1980-993X

Anagnostou E, Gianni A, & Zacharias I (2017). Ecological modeling and eutrophication—a review. *Nat. Resour. Model.*, *30*(3), e12130.

Bitencourt, LP, Fernandes, EH, Möller O, Ross, L (2020a). The contribution of ENSO cycles to the salinity spatio-temporal variability in a bar-built microtidal estuary. Reg. Stud. Mar. Sci. 40, 101496. https://doi.org/10.1016/j.rsma.2020.101496

Bitencourt LP, Fernandes EH, da Silva PD, Möller O (2020b) Spatio-temporal variability of suspended sediment concentrations in a shallow and turbid lagoon. J. Mar. Syst. 212. https://doi.org/10.1016/j.jmarsys.2020.103454

Bortolin EC, Weschenfelder J, Fernandes EH, Bitencourt LP, Möller OO, García-Rodríguez F, Toldo E (2020). Reviewing sedimentological and hydrodynamic data of large shallow coastal lagoons for defining mud depocenters as environmental monitoring sites. Sediment. Geol. 410, 105782. https://doi.org/10.1016/j.sedgeo.2020.105782

Caballero I, Fernández R, Escalante OM, Mamán L, Navarro G (2020) New capabilities of Sentinel-2A/B satellites combined with in situ data for monitoring small harmful algal blooms in complex coastal waters. Sci. Rep. 10, 1–14. https://doi.org/10.1038/s41598-020-65600-1

Carmichael, W. W. (1994). The toxins of cyanobacteria. *Sci. Am.*, *270*(1), 78-86.

Dall'Olmo G, Gitelson AA (2005) Erratum: Effect of bio-optical parameter variability on the remote estimation of chlorophyll-a concentration in turbid productive waters: Experimental results (Applied Optics (2005) 44 (412-422)). Appl. Opt. 44, 3342. https://doi.org/10.1364/AO.44.003342

de Souza MS, Muelbert JH, Costa LDF, Klering EV, Yunes JS (2018) Environmental Variability and Cyanobacterial Blooms in a Subtropical Coastal

Lagoon: Searching for a Sign of Climate Change Effects. Front. Microbiol. 9, 1–12. https://doi.org/10.3389/fmicb.2018.01727

Fernandes EHL, Dyer KR, Moller OO, Niencheski LFH (2002) The Patos Lagoon hydrodynamics during an El Niño event (1998). Cont. Shelf Res. 22, 1699–1713. https://doi.org/10.1016/S0278-4343(02)00033-X

Fernandes EHL, da Silva PD, Gonçalves GA, Moller OO (2021) Dispersion Plumes in Open Ocean Disposal Sites of Dredged Sediment. Water 1–20. https://doi.org/10.3390/w13060808

Fujita CC, Odebrecht C (2007) Short term variability of chlorophyll a and phytoplankton composition in a shallow area of the Patos Lagoon estuary (Southern Brazil). Atlântica 29, 93–106.

Howard A (2001) Modeling movement patterns of the cyanobacterium, Microcystis. Ecol. Appl. 11, 304–310. https://doi.org/10.1890/1051-0761(2001)011[0304:MMPOTC]2.0.CO;2

Jephcoat AP, Halliday AN (2008) Philosophical Transactions of the Royal Society A: Preface. Philos. Trans. R. Soc. A Math. Phys. Eng. Sci. 366, 4059–4060. https://doi.org/10.1098/rsta.2008.0221

Kardinaal WEA, Janse I, Kamst-Van Agterveld M, Meima M, Snoek J, Mur LR, Huisman J, Zwart G, Visser PM (2007) Microcystis genotype succession in relation to microcystin concentrations in freshwater lakes. Aquat. Microb. Ecol. 48, 1–12. https://doi.org/10.3354/ame048001

Kim M, Kim D, Kim J, Hong S, Shin KH (2021) Distribution of microcystins in environmental multimedia and their bioaccumulation characteristics in marine benthic organisms in the Geum River Estuary, South Korea. Sci. Total Environ. 757, 143815. https://doi.org/10.1016/j.scitotenv.2020.143815

Kjerfve B (1986) Comparative Oceanography of Coastal Lagoons. Estuar. Var. 63–81. https://doi.org/10.1016/b978-0-12-761890-6.50009-5

Lehman PW, Boyer G, Hall C, Waller S, Gehrts K (2005) Distribution and toxicity of a new colonial Microcystis aeruginosa bloom in the San Francisco Bay Estuary, California. Hydrobiologia 541, 87–99. https://doi.org/10.1007/s10750-004-4670-0

Marques WC (2012) The Temporal Variability of the Freshwater Discharge and Water Levels at the Patos Lagoon, Brazil. Int. J. Geosci. 03, 758–766. https://doi.org/10.4236/ijg.2012.34076

Matthiensen A, Beattie KA, Yunes JS, Kaya K, Codd GA (2000) [D-Leu1]Microcystin-LR, from the cyanobacterium Microcystis RST 9501 and from a Microcystis bloom in the Patos Lagoon estuary, Brazil. Phytochemistry 55, 383–387. https://doi.org/10.1016/S0031-9422(00)00335-6

Matthiessen A, Yunes JS, Codd GA (1999). De Cianobactérias No Estuário Da Lagoa Dos Patos , Rs. Rev. Bras. Biol. 59, 361–376.

Mishra S, Mishra DR (2012) Normalized difference chlorophyll index: A novel model for remote estimation of chlorophyll-a concentration in turbid productive waters. Remote Sens. Environ. 117, 394–406. https://doi.org/10.1016/j.rse.2011.10.016

Mobley, C. D. (1994). Light and Water: Radiative transfer in the natural waters. In Academic Press.

Möller OO, Castaing P, Salomon JC, Lazure P (2001) The influence of local and non-local forcing effects on the subtidal circulation of Patos Lagoon. Estuaries 24, 297–311. https://doi.org/10.2307/1352953

Möller OO, Castello JP, Vaz AC (2009) The effect of river discharge and winds on the interannual variability of the pink shrimp Farfantepenaeus paulensis production in Patos Lagoon. Estuaries and Coasts 32, 787–796. https://doi.org/10.1007/s12237-009-9168-6

Moller OO, Lorenzzentti JA, Stech JL, Mata MM (1996) The Patos Lagoon summertime circulation and dynamics. Cont. Shelf Res. 16, 335–351. https://doi.org/10.1016/0278-4343(95)00014-R

Odebrecht C, Abreu PC, Möller OO, Niencheski LF, Proença LA, Torgan LC (2005) Drought effects on pelagic properties in the shallow and turbid Patos Lagoon, Brazil. Estuaries 28, 675–685. https://doi.org/10.1007/BF02732906

Onyango DM, Orina PS, Ramkat RC, Kowenje C, Githukia CM, Lusweti D, Lung’ayia HBO (2020) Review of current state of knowledge of microcystin and

its impacts on fish in Lake Victoria. Lakes Reserv. Res. Manag. 25, 350–361. https://doi.org/10.1111/lre.12328

Paerl HW (2017) Controlling harmful cyanobacterial blooms in a climatically more extreme world: Management options and research needs. J. Plankton Res. 39, 763–771. https://doi.org/10.1093/plankt/fbx042

Possamai B, Vieira JP, Grimm AM, Garcia AM (2018) Temporal variability (1997-2015) of trophic fish guilds and its relationships with El Niño events in a subtropical estuary. Estuar. Coast. Shelf Sci. 202, 145–154. https://doi.org/10.1016/j.ecss.2017.12.019

Reichwaldt ES, Ghadouani A (2012) Effects of rainfall patterns on toxic cyanobacterial blooms in a changing climate: Between simplistic scenarios and complex dynamics. Water Res. 46, 1372–1393. https://doi.org/10.1016/j.watres.2011.11.052

Reynolds CS, Jaworski GHM, Cmiech HA, Leedale GF (1981) On the annual cycle of the blue-green alga Microcystis aeruginosa Kütz. emend. Elenkin. Philos. Trans. R. Soc. London. B, Biol. Sci. 325, 379–430.

Salomon OS, Yunes J S, Matthiensen A, Codd G A (2000) Does salinity affect the toxin content of an estuarine strain of Microcystis aeruginosa?. In: Xth International IUPAC symposium on Mycotoxins and Phycotoxins, 2001, Guarujá. Mycotoxins and Phycotoxins in perspective at the turn of the millennium - Proceedings of the Xth International IUPAC symposium on Mycotoxins and Phycotoxins p. 537-548.

Seiler, LMN, Fernandes, EHL, Siegle, E (2020). Effect of wind and river discharge on water quality indicators of a coastal lagoon. Reg. Stud. Mar. Sci. 40, 101513. https://doi.org/10.1016/j.rsma.2020.101513

Silva LM (2005) Ocorrência de Cianobactérias no Estuário e Costa Adjacente à Lagoa dos Patos, Rio Grande, RS: avaliação preliminar dos riscos À balneabilidade. FURG.

Soontiens N, Binding C, Fortin V, Mackay M, Rao YR (2019) Algal bloom transport in Lake Erie using remote sensing and hydrodynamic modelling: Sensitivity to buoyancy velocity and initial vertical distribution. J. Great Lakes

Res. 45, 556–572. https://doi.org/10.1016/j.jglr.2018.10.003

Spyrakos E, O'Donnell R, Hunter PD, Miller C, Scott M, Simis SGH, Neil C, Barbosa CCF, Binding CE, Bradt S, Bresciani M, Dall'Olmo G, Giardino C, Gitelson AA, Kutser T, Li L, Matsushita B, Martinez-Vicente V, Matthews MW, Ogashawara I, Ruiz-Verdú A, Schalles JF, Tebbs E, Zhang Y, Tyler NA (2018) Optical types of inland and coastal waters. Limnol. Oceanogr. 63, 846–870. https://doi.org/10.1002/lno.10674

Távora J, Fernandes EH, Bitencourt LP, Orozco PMS (2020) El-Niño Southern Oscillation (ENSO) effects on the variability of Patos Lagoon Suspended Particulate Matter. Reg. Stud. Mar. Sci. 40, 101495. https://doi.org/10.1016/j.rsma.2020.101495

Vaz AC, Möller OO, de Almeida TL (2006) Análise quantitativa da descarga dos rios afluentes da Lagoa dos Patos. Atlântica 28, 13–23.

Walstra, L.; Van Rijn, L; Blogg, H.; Van Ormondt, M. (2001). Evaluation of a hydrodynamic area model based on the COAST3D data at Teignmouth 1999. Report TR121-EC MAST Project No. MAS3-CT97-0086, HR Wallinford, UK, Pp. D4.1-D4.4.

Wynne TT, Stumpf RP, Tomlinson MC, Schwab DJ, Watabayashi GY, Christensen JD (2011) Estimating cyanobacterial bloom transport by coupling remotely sensed imagery and a hydrodynamic model. Ecol. Appl. 21, 2709–2721. https://doi.org/10.1890/10-1454.1

Xavier AC, King CW, Scanlon BR (2016) Daily gridded meteorological variables in Brazil (1980–2013). Int. J. Climatol. 36, 2644–2659. https://doi.org/10.1002/joc.4518

Yunes JS (2009) Florações de microcystis na lagoa dos patos e o seu estuário: 20 Anos de Estudos. Oecologia Bras. 13, 313–318. https://doi.org/10.4257/oeco.2009.1302.06

Yunes JS, Niencheski LFH, Salomon PS, Parise M, Beattie KA, Raggett SL, Codd GA (1998) Effect of nutrient balance and physical factors on blooms of toxic cyanobacteria in the Patos Lagoon , southern Brazil. Int. Vereinigung für Theor. und Angew. Limnol. 0770, 1796–1800.

https://doi.org/10.1080/03680770.1995.11901048